Distinct Metabolic Signatures Associated With Drought Response, Shoot Architecture And Flowering time In Camelina

Alice Vayssières, Stéphanie Boutet, Jean Chrisologue Totozafy, Frédérique Tellier, Michèle Winkler, Léa Barreda, Miriana Vicino, Anaïs da Costa, Massimiliano Corso, Jean-Denis Faure

Cover Page

Title:

Distinct Metabolic Signatures Associated With Drought Response, Shoot Architecture And Flowering time In Camelina

Running Head: Drought and Flowering Signatures In Camelina

Corresponding authors:

A. Vayssières
Université Paris-Saclay, INRAE, AgroParisTech, Institute Jean-Pierre Bourgin for Plant Sciences (IJPB)
78000 Versailles
France
+33 (0)1 30 83 32 74
alice.vayssieres@inrae.fr

J.D. Faure
Université Paris-Saclay, INRAE, AgroParisTech, Institute Jean-Pierre Bourgin for Plant Sciences (IJPB)
78000 Versailles
France
+33 (0)1 30 83 37 97
jean-denis.faure@agroparistech.fr

Subject areas: growth and development, environmental and stress responses

Number of colour figures: 7

Number of supplementary figures: 11

Number of supplementary tables: 5

Number of supplementary Datasets: 4

Title Page

Distinct Metabolic Signatures Associated With Drought Response, Shoot Architecture And Flowering time In Camelina

Drought and Flowering Signatures In Camelina

Alice Vayssières[1*], Stéphanie Boutet[1], Jean Chrisologue Totozafy[1], Frédérique Tellier[1], Michèle Winkler[1], Léa Barreda[1], Miriana Vicino[1,2], Anaïs Da Costa[1], Massimiliano Corso[1], Jean-Denis Faure[1*]

(1) Université Paris-Saclay, INRAE, AgroParisTech, Institute Jean-Pierre Bourgin for Plant Sciences (IJPB), 78000 Versailles, France (2) Department of Agricultural and Food Sciences (DISTAL), Università di Bologna - Alma Mater Studiorum, Viale G. Fanin 44, Bologna, 40127, Italy

* Corresponding authors:

Alice Vayssières
alice.vayssieres@inrae.fr

Jean-Denis Faure
jean-denis.faure@agroparistech.fr

Abstract

Camelina sativa is an ancient native oilseed species characterized by broad environmental adaptability, low-input requirements and tolerance to multiple stresses. Its potential use in agroecological transition with double cropping systems could be improved by breeding a shorter life cycle. However, this strategy should not compromise its resilience to stresses as well as its metabolite profiles and plasticity. The impact of flowering time on drought stress response and seed quality was evaluated in six camelina edited mutants, carrying combinatory mutations on the flowering time genes *SVP*, *TFL1*, *LHP1*, *ELF3* and *FLC* and leading to a range of flowering precocity and shoot architecture changes. We characterized the phenotype of these mutants in response to early and late drought and showed that their flowering time was not strongly altered contrary to branching and yield. Untargeted metabolomic demonstrated that in contrary to the lipidomic profile, the plasticity of the specialized metabolite was strongly modulated by drought in all genotypes. Specialized metabolite profile of the mutant seeds showed distinct pattern in response to drought with constitutive stress response of the bushy mutants in control condition including differences in antioxidant content such as glutathione, isoquercetrin, and coumaroyl quinic acid. Metabolite profiling in leaves also showed specific metabolic signatures of some mutants but with lower metabolite diversity than in seeds. Including additional genotypes with distinct flowering time, we identified metabolites correlating with this trait, such as vitamin B2 and kynurenic acid in seeds. These metabolites could be used as predictive markers of flowering time.

Keywords

Branching, Camelina, Drought response, Flowering time, Seed, Specialized metabolites

Introduction

The diversification of crops associated with a more sustainable cropping system could offer alternative solutions to mitigate climate change and support the agroecological transition. Camelina (*Camelina sativa* (L.) Crantz) is an oilseed crop of the Brassicaceae family producing oil enriched in polyunsaturated fatty acid, specifically the essential omega-3 polyunsaturated alpha-linolenic acid (Zanetti et al., 2021). Besides, camelina seeds accumulated other natural beneficial compounds, including tocopherols (vitamin E) as well as diverse specialized metabolites with antioxidant or antimicrobial activities (Barreda et al., 2025; Boutet et al., 2022; Budin et al., 1995; Quéro et al., 2016). These metabolites are characterized by large structural diversity and functions, and can be categorized into three main classes, namely phenylpropanoids, nitrogen-containing compounds and terpernoids (Barreda et al., 2024). Camelina is also characterized by its low agricultural input requirement and its resilience upon biotic and abiotic stresses and is therefore used in relay cropping or as catch crop (Zanetti et al., 2021). However, its use in double or relay cropping in particular during summer was restricted due to several limitations, mainly late maturity and high occurrence of annual weeds (Leclère et al., 2018). In addition, variable water availability after sowing caused heterogenous seedling emergence. Using camelina as a catch crop would require the improvement of three main traits: (1) its life cycle with early flowering phenotype to allow full seed maturation, (2) its plant architecture with enhanced bushiness to compete with weeds, and (3) its tolerance to drought and heat during the entire life cycle.

The fine-tuning of flowering transition determines the timing of seed set and subsequently the reproductive success. The transition from vegetative to reproductive growth is a complex and tightly controlled process that involves a combination of endogenous and environmental signals (Andrés and Coupland, 2012). In the Brassicaceae model plant *Arabidopsis thaliana*, which is closely related to camelina, multiple pathways including vernalization, photoperiod, circadian clock, sugar, age, thermosensory, autonomous, and gibberellin, target integrator genes interconnected in a complex genetic network (Andrés and Coupland, 2012). The regulation of drought stress responses in plants involves also complex signaling networks and flowering time regulators that are known to play a role in coordinating these responses (Kazan and Lyons, 2016). Notably, the flowering repressor SHORT VEGETATIVE PHASE (SVP) confers drought resistance while the mutation of flowering activator *LIKE HETEROCHROMATIN PROTEIN 1* (*LHP1*), showed drought resistance in Arabidopsis (Bechtold et al., 2016; Ramirez-Prado et al., 2019; Wang et al., 2018). Inversely, drought strongly impacts several physiological traits including the reduction of plant biomass but also flowering time (Bacelar and Aroca, 2013). Drought induces rapid plant development leading to early flowering in *A. thaliana* and its close related species *Brassica rapa* (Cho et al., 2017; Franks et al., 2007). This strategy, also called drought escape, is often at the expense of plant yield. The trade-off between drought escape and yield may vary among plant species and depend on the specific environmental conditions. For example, studies in wheat have shown that early flowering induced by drought could be favorable for yield (Shavrukov et al., 2017). Conversely, in other species such as rice, maize and quinoa, drought increases the number of days to flower (Abrecht and Carberry, 1993; Fukai, 1999; Geerts et al., 2008). The regulations of seed quality and flowering time are also closely interconnected, as the timing of flowering significantly influences seed development. A direct regulation of various seed traits, including seed size,

dormancy, longevity and quality by key flowering regulators have been demonstrated in various plant species. (Nadal Bigas et al., 2025; Ohto et al., 2005; Shoesmith et al., 2021; Soppe et al., 2021; Zhang et al., 2020). Understanding the link and interaction between flowering, drought and seed quality in camelina is essential for developing crops with improved resilience to environmental challenges in the context of climate change.

The mechanisms underlying the regulation of flowering time in camelina, as well as its pleiotropic roles in drought stress response and seed quality, remain poorly understood. Genome wide association study (GWAS) demonstrated the high heritability of flowering time in camelina and identified significant trait-associated single nucleotide polymorphisms (Luo Lily et al., 2021). In addition, in camelina one out of four quantitative trait locus (QTL) associated with flowering time overlaps with seed-size-related QTL (Li et al., 2021). Unfortunately, the low genetic diversity of camelina populations associated with its highly redundant hexaploid genome limit the breeding potential of this crop (Kagale et al., 2014). A low-to-moderate predictive ability to improve early flowering traits was observed in camelina (Luo Lily et al., 2021). Using multiplex-editing, a previous study took advantage of the hexaploid genome to obtain a wide range of mutations on the three homoeologs of the flowering repressor genes *FLOWERING LOCUS C* (*FLC*), *SVP*, *LHP1*, *TERMINAL FLOWER 1* (*TFL1*) and *EARLY FLOWERING LOCUS 3* (*ELF3*) (Bellec et al., 2022). This strategy induced combinatorial mutations associated with early flowering phenotype, determinate flowering, shorter stature and/or basal branching (Bellec et al., 2022). These *flo*- mutants could therefore represent a valuable genetic background for alternative summer catch crop varieties.

To further elucidate the impact of summer cropping on these early flowering *flo*- mutants, we characterized mutant phenotypes in response to early and late drought. We also compared the impact of early and late drought on seed quality and identified different responses across genotypes. Untargeted metabolomic and lipidomic analyses were carried out on seeds to investigate whether flowering mutations could modify seed metabolome profiles upon drought. Our analysis indicates no significant impact of drought on the lipidome contrary to the specialized metabolome in both control and mutants. In addition, in seeds of the bushy *flo*- mutants grown under control conditions, we observed a specialized metabolome associated with drought response. By comparing the *flo*- mutants with additional camelina accessions, we identified metabolites that could be used as predictive markers of flowering time in seeds and leaves.

Results

Drought impacts strongly the flo- *branching phenotype but slightly the flowering precocity*

We selected six mutants among the previously described camelina *flo*- mutants that show a range of early flowering, determinate growth and branching phenotypes (Bellec et al., 2022; Figure 1, Figure S1A). The *flo*- mutants were subjected to two different drought stresses, before flowering (stress 1) or during flowering at seed set (stress 2). Early drought (stress 1) was used to evaluate the impact of water limitation on flowering time and lateral shoot formation. We monitored the soil water content (SWC) with control plants at 50% SWC and early

drought stress was applied on 2 week-old plants (Figure S1B–C). By examining the morphology of the shoot apical meristem, we observed that at this stage none of the meristems of the mutants carried flowers. However, the meristems of the *B1-2* and *C2-19* mutants showed leaf primordia with axillary meristems in their axils, suggesting that they had undergone floral transition (Grbić and Bleecker, 2000; Figure S2). Water loss was conducted until 15% SWC for which wilting was observed (40-80% of the plants at day 22, 26 and 29; Figure S1C–D) and these stress conditions were maintained for 10 days. We measured the leaf water content (LWC) before water loss (T0), during water loss (day 12), at the end of the stress period (day 30) and 4 days after the recovery to 50% SWC (day 34) (Figure S1E). At the end of the stress 1, significant decrease in LWC was observed in all genotypes (Figure S1E). There was no significant difference of LWC between wild type and *flo*- mutants in control conditions, at the end of the drought period (day 30) and during recovery (day 34). However, the *C2-19*, *B23-3* and *A4-12* mutants showed transient tolerance to water loss at day 12, with no significant LWC reduction while Celine and the other *flo*- mutants showed a significant decrease in LWC already (Figure S1E). Together, these data showed a strong impact of the stress on all genotypes tested and suggest that the *C2-19*, *B23-3* and *A4-12* mutants may be more tolerant to mild drought.

The *flo*- mutants showed, as expected, early flowering time from 39.5 days for *B1-2* to 49.3 days for *A1-14* compared to wild type Celine (55.6 days) (Figure 1B, Table S1). The observation of the meristem fate in control condition confirmed the early flowering transition in the *flo*- mutants (3 weeks for *A40-24*, *B1-2* and *C2-19*; 4 weeks for *A1-14*, *A4-12* and *B23-3*) compared to wild type Celine (5 weeks) (Figure S2). Early drought induced a decrease in flowering time of 3.2 days for wild type plants but impacted differently the *flo*- mutants (Figure 1B). *C2-19*, *A40-24* and *A1-14* mutants showed reduced flowering time upon stress similar to wild type (2.6, 3.3, 3.6 days). *B1-2*, *B23-3* and *A4-12* however did not show any significant modification of flowering time in response to early drought stress. Reduction of flowering time was most probably due to a modification of flower emergence and not floral transition since no difference of total leaf number could be observed in all genotypes except for *A1-14*, the less precocious mutant (Figure S3A). Among the *flo*- mutants, *A1-14* and *A4-12* were characterized by their increased number of basal branches compared to wild type (Figure 1A). Branch number was defined at the end of the stress period when wild type camelina still did not have any inflorescence. *B23-3* enhanced branching was caused by an increase in inflorescence branches rather than basal branches (Figure 1A and C and Figure S3B). Interestingly, drought stress strongly reduced the total number of branches (inflorescence and basal) for all *flo*- mutants except for *B1-2* that had the lowest branch number (Figure 1A and Figure S3B). Altogether, our results showed that early drought stress during development strongly impacted the *flo*- branching trait but only mildly flowering time.

Early and late drought stresses showed constrasting impact on seed yield in wild type and the flo- *mutants*

Early drought stress induced in wild type a significant reduction of plant height, total seed number and seed yield while increasing thousand seed weight (Figure 2, Figure S4). A similar response for plant height and seed yield could be observed in the *flo*- mutants except for *B1-2,* the shortest genotype (Figure 2A–B). However, except for *A4-12*, thousand seed weight did not increase in *flo*- mutants upon stress and even slightly decreased for *B23-3*

(Figure 2C). The contrasting responses on seed traits between wild type and *flo*- mutants could be explained by the fact that the *flo*- mutations already had a strong impact on seed yield, from -80.4% for *B1-2* to -16.9% for *A1-14* in control conditions (Figure 2B). To better evaluate the impact of drought stress on seed yield and quality, we carried out a second drought experiment (stress 2) that started when plants had open flowers. For this purpose, the 10-day drought at 15% SWC was carried out on 6 week-old plants for the *flo*- mutants and on 8 week-old plants for the Celine wild-type so that drought would be occurring during seed set (Figure S1B, F–G). The transition from 50% SWC to 15% SWC was slower for the *flo*- mutants (12 days) compared to Celine (3 days) (Figure S1B). Wilting was also more severe in stress 2 for both the *flo*- mutants (100% at day 17 and 20) and Celine (100% at day 26 and 31) compared to stress 1, most probably caused by the larger plant size (Figure S1F–G). Stress 2 had a lower impact on wild type plant height compared to stress 1, as it was applied later in development. On the contrary, most *flo*- mutants showed similar plant height in stress 1 and stress 2 experiments except for *B23-3*, the tallest mutant (Figure 2A). Notably, *flo*- mutants and wild type seed yield was significantly reduced by drought, both stress 1 and 2 or exclusively by stress 2, except for *B1-2* that was not impacted by water deficiency (Figure 2B). Stress 2 had less impact on total seed number compared to stress 1 and did not lead to thousand seed weight increase in both wild type and *flo*- mutants (Figure 2C and Figure S4). The *B23-3* mutant even showed a lower thousand seed weight in stress 2 compared to the control (Figure 2C). In conclusion, drought at flowering (stress 2) had a stronger impact on seed yield in the *flo*- mutants than earlier in development (stress 1). Therefore, to investigate seed quality, the analysis was only performed on seeds from stress 2 plants.

Lipidomic profile of wild type and flo- *seeds after drought stress*

To understand how drought could impact lipid profile characterized by high polyunsaturated fatty acid content in camelina seeds, we first used a targeted approach to quantify fatty acids in wild type and the *flo*- mutants. While no difference was observed in total fatty content (Figure S5A), principal component analysis (PCA) of the fatty acid composition showed that axis 1 accounting for 39% of the variance, discriminated between the bushy *A1-14* and *A4-12* mutants and the other genotypes (Figure S5B). Notably, these mutants accumulated significantly more saturated fatty acids (C18:0, C20:0 and C22:0) than the wild type in control conditions (Figure S5C, Data S1). However, these differences represented less than 1% of the total fatty acids (Figure S5D). Next, untargeted lipidomic was carried out on control and stressed seeds of wild type and the *flo*- mutants identifying 252 lipids with a putative annotation (Data S2). PCA was able to discriminate genotypes in axis 2 accounting for 11% of the variance, with three main groups, (i) wild type with *A40-24*, *B1-2* and *C2-19,* (ii) *B23-23,* and finally (iii) *A1-14* with *A4-12* (Figure 3A). ANOVA simultaneous component analysis (ASCA) could not discriminate an effect of the drought stress (p=0.07) while the genotypes were more discriminants (p=0.01). A total of 79 (30.7%) lipids were differentially accumulated across all conditions (Figure 3B and Table S2). A very minor part of the lipidome, between 1.1% for *C2-19* and 7.1% for *A4-12*, was differentially accumulated upon stress (Figure 3B). Hierarchical clustering of the 79 differentially accumulated metabolites identified two main clusters (cluster 1 and 2) that could be separated in six different subclusters defining specific lipid families (Figures 3C–D). Cluster 1A represented mostly by sphingolipids showed a higher and constitutive accumulation in *B23-3* mutant

compared to the other genotypes. Similarly, the lipids of cluster 1B that included mainly phospholipids and galactolipids were accumulated in *B23-3* and in the branched mutants *A4-12* and *A1-14*. Interestingly, these lipids were also reduced in wild type by the presence of drought (Figure 3D). Phospholipids, mostly represented in cluster 2A, were strongly impacted by the mutations for flowering genes. They were less accumulated in all *flo-* mutants, particularly in *C2-19*, *B23-3*, *A1-14* and *A4-12*, compared to wild-type seeds. Members of the Alkyl Hydroxycinnamates (AHC) family, known to be involved in cuticles and suberin, defined the cluster 2B and also, showed reduced content in *B23-3* and in the bushy mutants *A1-14* and *A4-12* compared to wild type (Figure 3D). Finally, clusters 2C and D containing mostly glycerolipids also discriminated the two bushy mutants (Figure 3C). In conclusion, drought stress led to limited but specific changes in seed lipid content in both wild type and *flo-* mutants. Notably, the *A1-14, A4-12* and *B23-3* mutants showed specific lipidomic changes compared to wild-type in both control and drought conditions.

flo- *seed specialized metabolome is shaped by drought stress*

Since specialized metabolites are known to be involved in abiotic stress responses (Nakabayashi et al., 2014; Boutet et al., 2022; Barreda et al., 20252024) untargeted metabolomic analysis was also carried out on mature seeds produced in the late drought experiment (stress 2) of wild type and *flo-* mutants. We identified 1761 metabolic features accumulated in seeds from wild type camelina and *flo-* mutants among which 1277 (72.5%) were differentially accumulated across genotypes and/or growing conditions (Data S3 and Table S3). The PCA on axis 1 (29% of variance) separated partially the *A1-14* and *A4-12* mutants to the other genotypes. Axis 2 discriminated control and stressed samples but in an opposite direction for *flo-* mutants and wild type (Figure 4A). Contrary to the lipidomic dataset, the result of the ASCA for specialized metabolome showed a significant effect of both genotypes and drought stress ($p<0.05$). First, we analyzed the metabolomic response to drought in the different genotypes. In wild type seeds, 202 features were differentially accumulated in response to stress from which only 38 were genotype specific (Figure 4B, blue arrow). Eleven features including putative sinapic acid and two putative flavonoids were specifically modulated in response to drought in all *flo-* mutant seeds while not responding in wild type seeds (Figure 4B, red star; Figure S6). Clustering of the genotypes with the 202 wild type differentially accumulated features highlighted three accumulation patterns (Figure S7): mutants that followed the wild type response (*A40-24* and *B1-2*), mutants that showed the wild type stress response in control condition (*A1-14* and *A4-12*) and mutants that showed a control response in stress condition (*C2-19* and *B23-3*). Hierarchical clustering of the features identified two main clusters (Figure 4C). Cluster 1 accounted for 64 features accumulated in stressed wild type and *B1-2* and *A40-24* but constitutively accumulated in the bushy mutants *A4-12* and *A1-14* (Figure 4C–D) and characterized by the presence of putative flavonoids (isoquercetrin), a putative cinamate-ester (coumaroyl quinic acid), a phenolic coumpoud (p1121) and four lipids (palmitamide, 1-Hexadecanoyl-sn-glycerol, dilinolenin and 9-octadecenamide) (Figure 4E). Cluster 2 could be separated in three different subclusters. Cluster 2A, including 34 features, showed an opposite pattern of cluster 1 with features that were depleted in stressed wild type and with different mutant responses ranging from no response (*C2-19*) to constitutively stressed (*A4-12*) (Figure 4F). This cluster was characterized by glutathione and a putative

glucosinolate (Figure 4G). The two remaining clusters 2B and C showed a more complex pattern associated with the individual genotypes (Figure 4C). Altogether, our data showed that the *flo-* mutants have specific metabolomic changes compared to wild type after drought stress including constitutive stress response of the bushy mutants.

Metabolomic and lipidomic integration identified limited but specific lipid and secondary metabolite correlations

To understand whether the changes in secondary metabolites may be linked to lipid adjustments, we integrated both specialized metabolite and lipid datasets, using sparse partial least square discriminant analysis (sPLS-DA) for two omics integration (Figure S8A, Rohart et al., 2017). Arrow sample plot from the sPLS-DA, showing how each sample project in both, lipid (arrow start) and specialized metabolites (arrow end), indicated low agreement at the sample level observed for both genotypes (Figure 5A) and response to drought (Figure S8B). Putative lipids and specialized metabolites that define each component were represented in the correlation plot (Figure S8C, correlation coefficient>0.55) and clustered in two networks with a limited number of lipid-metabolite correlations (Figure 5B, correlation coefficient>0.55). The first network accounted for lipids and specialized metabolites that explains the separation of the *A1-14* and *A4-12* bushy mutants from the other genotypes, included two putative nitrogen-containing compounds (p771 and p769) and an unknown feature (p772) and seven triglycerides (Figure 5B). The second network, that strongly participated to the separation of component 2 (Figure S8A), discriminating partially control and stressed samples, showed negative correlations between the putative HydroxyCinnamic Acid (HCA), sinapoyl-glucose (p74) and siribinose A6 (p178) and the Alkyl HydroxyCinnamates (AHCs), C18:1-coumarate (n15), C18:2-coumarate (230) et C19:1-coumarate (n104) (Figure 5B–C). Altogether, these results suggest that lipid remodeling is largely independent from changes in secondary metabolism. However, specific adjustments in the accumulation of alkyl hydroxycinnamates and hydroxycinnamic acids may occur in response to drought.

Specialized metabolite landscape of edited flowering mutant seeds and leaves

To further explore the impact of early flowering mutations on specialized metabolite profiles, we analyzed the 725 seed metabolic features that were differentially accumulated among genotypes in control condition (41% of the total metabolites quantified, Table S4). Enrichment analysis did not allow the identification of profound modification on metabolite family or family group in this list (Figure S9A–B, Table S4). The hierarchical clustering of these features highlighted two groups of genotypes with the bushy mutants *A1-14* and *A4-12* in group 1 and the remaining genotypes in group 2, validating that mutations in different genes affecting both flowering time and shoot architecture revealed a highly specific seed metabolic signature (Figure S10A). The twenty most discriminating features between these two groups were identified by sPLS-DA component 1 (22% of the variance) (Figure 6A and Table S5). Out of the 20 features, three were annotated as putative flavonoids (isorhamnetin 3-rutinoside, isoquercetrin) and lipid (palmitamide) (Figure 6B). Since florigen is synthesized in leaves, we also investigated whether *flo-* mutants have specific specialized metabolic responses in these tissues. A total of 913

features were identified, among which 132 (14.5%) were differentially accumulated across genotypes highlighting lower inter-genotype metabolic diversity in leaves compared to seeds (Data S4, Table S4). In this tissue as well, no significant enrichment of metabolic families could be detected (Figure S9C–D, Table S4). Unlike seeds, hierarchical clustering identified three groups with wild type and *A40-24* (group I) having an opposite pattern of accumulation than *A4-12* and *A1-14* (group II). The *B1-2, C2-19* and *B23-3* mutants (group III) showed a more complex pattern of accumulation (Figure S10B). The sPLS-DA ran with these groups, showed that component 1 (24% of the variance) was able to discriminate between the wild type and *A40-24* group from the other genotypes (Figure 6C). Component 2 (9% of the variance) discriminated against the bushy mutants from the *B1-2*, *C2-19* and *B23-3* (group III). Out of the twenty most discriminating features of component 1 only ferulic acid could be annotated (Figure 6D and Table S5). In conclusion, the *flo-* mutants showed specific metabolic signatures both in seeds and in leaves with higher metabolite variation among genotypes in seeds compared to leaves. In both tissues, the differences in metabolite profiles mainly reflected the diverse combinations of complex mutations and were not associated with flowering time.

Identification of specialized metabolites in seeds and leaves correlated with flowering time

To identify metabolite features specifically correlated with flowering time, we explored the metabolome of late- and early-flowering natural accessions of camelina in addition to the *flo-* mutants (Figure S11A–B). The CAM151 plants showed similar flowering time than the wild type accession Celine (56.6 days), while CAM203 flowered later at 67.2 days and CAM221, CN101981 and L2F4 flowered earlier like the latest *flo-* mutants (Figure S11B). These accessions did not show strong modifications in shoot architecture (Figure S11A). The seed yield showed the same differences across the genotypes compared to flowering time (Figure S11C). Untargeted lipidomic and metabolomic analyses were carried out in seeds and leaves of these accessions and the PCA analyses showed that the *flo-* mutants were always grouped with wild type compared to the natural accession lines with the exception of L2F4 that clustered with *flo-* mutants for leaf specialized metabolites (Figure 7A–C). These results demonstrate that the *flo-* mutants have a specific metabolome that was closer to the wild type accession Celine, from which they originate, than the other accessions even if they share similar flowering time. By combining all the data together with all the different genotypes, correlation network analysis of metabolic changes confirmed the high correlation between flowering time and yield with a Pearson correlation coefficient of 0.92 (Figure 7D and F). In seeds, two and six metabolites were respecetively positively and negatively correlated with flowering time and only two with yield (Figure 7D). Flowering time was positively correlated with sucrose content while negatively correlated with putative kynurenic acid and putative vitamin B2 (riboflavin) in seeds (Figure 7E). Interestingly, a different network was found in leaves with seven interconnected metabolites that were negatively correlated with flowering time and one negatively correlated with yield from which none were annotated (Figure 7F). These metabolites could be therefore used as predictive markers of flowering time in vegetative tissues.

Discussion

The use of camelina in summer intercropping or relay cropping could be at risk of adverse growing conditions in particular with drought during vegetative and flowering stages as well as suboptimal conditions during seed maturation. The latter risk could be mitigated by shortening camelina flowering time but not at the expense of drought tolerance. Severe early-stage drought induced a reduction of flowering time in camelina as shown previously for other Brassicaceae such as Arabidopsis or *Brassica rapa* with respectively 2–3.8 days and 1.9–8.5 days precocity (Franks et al., 2007; Riboni et al., 2013). Similar drought escape strategy was observed in camelina (3.2 days for wild type plants) albeit this crop was naturally tolerant to many abiotic stress (Enjalbert et al., 2013; Gugel and Falk, 2006; Zanetti et al., 2017). In *B. rapa*, plants escape drought by flowering early rather than by increasing water use efficiency and this response could be inherited through natural selection in multiyear drought conditions (Franks, 2011; Franks et al., 2007; Rathnayake and Parachnowitsch, 2025).

The flowering time observed for all the *flo-* mutants and natural camelina accessions was strongly correlated with reduced seed yield in both control and drought conditions. This negative correlation between flowering time and seed yield was also observed in Arabidopsis (Gnan et al., 2014). Branching was also associated with seed yield reduction in two out of the seven *flo-* mutants as observed in arabidopsis or during maize domestication (Doebley et al., 1997; Gnan et al., 2014). Notably, an increase in thousand seed weight in response to drought applied at an early developmental stage was observed, as previously been reported in camelina (Alberghini et al., 2025). Increased thousand-seed weight was also detected in some *flo-* mutants under control conditions, consistent with the larger seed size previously described in some of them (Bellec et al., 2022). As the total number of seeds produced was drastically reduced in both the *flo-* mutants and the wild type under early drought stress, the increase in thousand seed weight may reflect a compensatory mechanism leading to a higher assimilate allocation per seed. While seed yield is a secondary trait for cover cropping strategy, the ability to grow camelina in intercropping conditions would very much rely on its ability to be competitive against weeds (Leclère et al., 2018). In the *flo-* bushy mutants *A4-12* and *A1-14,* the branching phenotype was completely abolished upon drought stress, potentially limiting the use of this trait in the field. Nonetheless, in all mutants, flowering precocity was not associated with enhanced sensitivity to severe drought conditions (15% SWC). In intermediate drought conditions (25% SWC, during water lose), Leaf Water Content (LWC) was not changed compared to control conditions in three mutants (*C2-19*, *B23-3*, *A4-12*) contrary to wild type suggesting a potential tolerance of these genotypes to milder drought. Altogether, our results indicate that the *flo-* mutants are good candidates for relay cropping during summer as they most certainly be able to complete their life cycle before autumn in field condition. However, the loss of the bushy phenotype upon drought could limit its ability to control weed development.

The great potential of camelina in intercropping relies not only on its cover crop ability but also on its oil and co-product production (Zanetti et al., 2021). It was therefore important to assess the effect of drought and precocity on seed lipid profile as well as specialized metabolites in both seeds and leaves. The environmental effect on

fatty acid profile in camelina were reported as important (Brock et al., 2020; Raziei et al., 2018; Vollmann et al., 2007) or moderate to low (Boutet *et al*., 2022) most likely depending of the field conditions and the nature of abiotic and abiotic stress occurring during the trials. Here we showed that drought stress did not have an important effect on seed lipid fatty acids even in *flo*- mutants indicating that flowering precocity like water restriction were not impacting oil quality in camelina. Nonetheless, the *flo*- mutants showed specific changes in some lipid families like phospholipids in particular polyunsaturated medium chain phosphatidylcholine (PC38.5, PC38.4, PC36.6 PC34.4, PC34.6). Remodeling of cell membranes are often observed in response to abiotic stresses such as drought in particular for thylakoid membranes allowing a structural re-shaping and maintenance of chloroplasts function and photosynthetic energy supply both in leaves like in seeds (Gasulla et al., 2013; Torres-Franklin et al., 2007 Ferreira et al., 2021). Notably, the ratio between polyunsaturated and saturated fatty acids is enhanced to improve membrane fluidity protecting cells from damage (Gigon et al., 2004; Upchurch, 2008).

By contrast, specialized metabolites were strongly affected by drought stress in the different genotypes (72.5% of quantified metabolites) with specific responses, confirming previous work in field experiment (Boutet *et al.*, 2022). The *flo*- mutants showed differential stress response for their seed specialized metabolites. The bushy mutants *A1-14* and *A4-12* constitutively accumulated stressed wild type metabolic profile while *C2-19* and *B23-3* mutants did not show any wild type stress response. The last two mutants, *A40-24* and to lesser extent *B1-2,* were having the same specialized metabolic signature as wild type. The constitutive drought signature observed in the seeds of the *A1-14* and *A4-12* mutants is most likely not associated with their flowering precocity, as drought appeared to have only a minor effect on flowering time, and the *flo*- mutants showing the greatest precocity did not display a constitutive drought signature. This constitutive stress signature may result from reduced carbon allocation to seeds, likely due to the high number of lateral shoots in these plants, a phenomenon also described in other Brassicaceae species (Bennett et al., 2012; Van Daele et al., 2012).

Specialized metabolite signature of the drought response in wild type seeds included glutathione, the flavonoid isoquercetrin, the cinnamate ester coumaroyl quinic acid and modified lipids like dilinolenin, 1-hexadecanoyl-sn-glycerol and 9-octadecenamide. Notably, several of these metabolites are strong antioxidants known to be involved in abiotic stresses (Rai et al., 2023; Soviguidi et al., 2022). In particular, glutathione was accumulated upon drought in seeds in wild type but constitutively accumulated in the *A1-14* and *A4-12 flo*- mutants. Glutathione has been involved in drought tolerance in Arabidopsis in particular by inducing translational changes in hormonal and stress-signaling pathway (Cheng et al., 2015). Eleven metabolites, including sinapic acid, were specifically accumulated upon drought in seeds in *flo*- mutant while not modulated by stress in the wild type. Many abundant cinnamic acids in Brassicaceae seeds derive from sinapic acid core structure and decorated metabolites, mainly sinapate esters (COO-R) (Baumert et al., 2005; Boutet et al., 2022; Corso et al., 2020). Sinapic acid and sinapate esters were involved in a wide range of stress responses in Brassicaceae species, including reduction of oxidative stress damage and UV-stress (Milkowski and Strack, 2010). In addition, cinnamic acids, including sinapic acid and some derivatives, showed a strong antioxidant and antibacterial activity against plant

and human pathogens (Engels et al., 2012; König et al., 2014; tesaki et al., 1998). Glutathione and sinapic acid or its derivatives were described to interfere with abscisic acid (Bi et al., 2017; Cheng et al., 2015). It is also well described that abscisic acid is involved in shoot branching, presenting a putative explanation for the differences in these metabolite levels in the bushy mutants *A1-14* and *A4-12* (Yao and Finlayson, 2015).

In leaves, ferulic acid was lower in all *flo*- mutants but *A40-24* compared to wild type. Ferulic acid is one of the most abundant HydroxyCinnamic Acid (HCA) in plants and its accumulation is correlated with drought resistance in wheat and barley (Hura et al., 2009; Piasecka et al., 2017). The HCA are metabolites involved in cell wall structures by covalently binding to hemicellulose arabinoxylans improving plant rigidification and limiting water loss (Zeiss et al., 2021). We also observed specific changes in other HCA derivatives Alkyl HydroxyCinnamates (AHC), C18-ferulate, C16-coumarate, C15-coumarate, C17-ferulate in particular in the *A1-14* and *A4-12* bushy mutants. In camelina, AHC were previously characterized as predominantly alkyl coumarates and alkyl caffeates (Razeq et al., 2014). The AHC are present in suberin-associated waxes and cuticular waxes that are important components for preventing water loss (Delude et al., 2016; Lee et al., 2014). Seeds AHCs were reduced in the branched *flo*- mutants and could therefore impact seed quality (Vishwanath et al., 2013). The adjustment between specific HCA and AHC was also pointed out in the metabolome and lipidome integration analysis, indicating potential cross-regulation between these lipids and the phenylpropanoid pathway in response to drought. Overall, the integration of lipidomic and metabolomic data suggests that lipid remodeling is largely independent of changes in secondary metabolism. This result was expected, since drought exerted a stronger influence on the modulation of specialized metabolites than on lipid composition in seeds.

Finally, including additional genotypes with distinct flowering time but without major change in shoot architecture, we identified metabolites strongly correlating with this trait. As expected, sucrose was correlated with flowering time as observed in many species (Cho et al. 2018). But except for hormone metabolism and carbohydrate availability, there is limited information regarding the specialized metabolic changes that take place at floral transition (Wahl et al., 2013, Izawa, 2021; Praena Tamayo et al., 2022). Our results indicate a correlation between flowering time and several putative specialized metabolites including vitamin B2 and kynurenic acid, a tryptophan catabolite in seeds.

In conclusion, the early flowering phenotype observed in the edited camelina lines did not modify their tolerance to drought but revealed specific changes in specialized metabolites. These changes were however far less extended than those observed in camelina natural diversity (Figure 7). The camelina *flo*- mutants represent nonetheless valuable genetic resources for summer intercropping and their potential use would still need to be validated in open field trials.

Materials and Methods

Plant material and growth conditions

The experiments were performed using camelina (*Camelina sativa*) cultivars Celine, CAM221, CAM151, CAM203, from the BAZ, Braunschweig Genetic Resources Centre, CN101981 from Canadian Plant Gene Ressources of Canada (GRIN-Global-CA), the recombinant line L2F4 from the INRAE breeding program GENESYS PIVERT Probioraff and the *C2-19, B1-2, B23-3, A40-24 A4-12* and *A1-14* mutants described in Bellec et al., (2022). These mutants are in the Celine genetic background and we name them "*flo*- mutants" because of their different combinations of mutations in flowering time genes *CsFLC*, *CsSVP*, *CsLHP1*, *CsTFL1* and *CsELF3* (Bellec et al., 2022, Figure S1A). Seeds were germinated first on paper disk in Petri dishes for 4 days before transferring the seedlings to soil in a long day (LD, 16 h light: 8 h dark) glasshouse supplemented with artificial light when necessary, with 24 °C day and 13 °C night temperatures. For the drought experiments, soil water content (SWC) was estimated using pot weight. For this purpose, all 14-cm ⌀ pots of both early (stress 1) and late (stress 2) drought experiment were filled with 800 g of soil. Ten pots were used as control pots to calculate pot weight at 100% SWC and 0% SWC as follows. Pots were first soaked into water and we let the water run out of the pot by gravity for 1-hour to estimate pot weight at field capacity (100% SWC). The same pots were subsequently dried using a dry oven to estimate their weight at 0% SWC. The percentage of SWC across the experiment was calculated subsequently: % SWC = ((pot weight - weight at 0% SWC) / weight at 100% SWC) x 100. The pot weight was corrected in the experiment to account for plant weight. For this purpose, shoots of control plants were harvested and weighted at 5 weeks (3g), 6 weeks (7g) and 8 weeks (25g). For early drought experiment (stress 1), seedlings were first watered 12 days until all pots reached 50% SWC, then control plants were kept at a 50% SWC while stress plants were water deprived until 15% SWC and maintained at 15% SWC for 10 days before recovering 50% SWC for 3 days (Figure S1B–C). Later, plants were watered without monitoring the % SWC. The late drought experiment (stress 2) was carried out at flowering (Figure S1B). For this purpose, the 10-day drought at 15% SWC was carried out on 6 week-old plants for the *flo*- mutants and on 8 week-old plants for the Celine wild-type (Figure S1B and F). In this drought experiment, recovery was not monitored and the three last days of the Celine control had SWC ranging from 73% to 93% while it was maintained at 50% for the *flo*- control. Control plants were the same in both drought experiments (stress 1 and stress 2). Cultivars CAM221, CAM151, CAM203, CN101981 and L2F4 were cultivated in the same control condition at the same time.

Plant phenotyping

Wilting was monitored using visual observation of the plant. Plant was considered wilted if at least one leaf was wilted. The percentage of whole-leaf water content (%LWC) was calculated as follow: %LWC = ((leaf fresh weight – leaf dry weight) / leaf fresh weight) x 100. Day to flowering was scored at the first flower openning. The branch number and length were carried out at the end of the stress 1, on 6 week-old plants. Final plant height was measured when plants were completely dried. Thousand seed weight was counted using an elmor C3 seed counter. At least 10–12 plants were used for each condition.

Confocal laser scanning microscopy

Shoot apices of Celine and *flo-* mutants were dissected under a stereomicroscope at 2, 3, 4 and 5 weeks after sowing and fixed with 4% paraformaldehyde (PFA). The samples were vacuum-infiltrated twice for 10 min each and transferred to fresh PFA at 4°C overnight before clearing with ClearSee (Kurihara et al., 2015) for 3 to 7 days. Cell wall was dyed using 0.1% (v/v) SCRI Renaissance 2200 (Musielak et al., 2015) one day before imaging and imaged with an SP8 (Leica Microsystems) using excitation wavelength: 405 nm; detection wavelength: 410–510 nm. At least 3–6 plants were observed under the stereomicroscope for this experiment.

Extraction, quantification and annotation of lipid and specialized metabolites fractions

Mature dry seeds and leaves from vegetative plants of Celine, CAM221, CAM151, CAM203, CN101981, L2F4 and the *flo-* mutants in control condition and mature dry seeds of Celine and the *flo-* mutants under drought stress were used in this experiment. For this purpose, flowers were marked individually on the first day of opening on the starting day of the drought period (stress 2) and on the same day in the control plants (Figure S1F). Mature dry seeds from three marked siliques of three plants were pooled and grinded using a HG-600 Geno/Grinder® 2010. Leaves number four were harvested in vegetative plants at four weeks after sowing. Leaves from three plants were pooled for each replicate, dry freeze in liquid nitrogen and ground using SK350 paint shaker. Metabolites were extracted from 30 mg of mature dry seeds or 200 mg of leaves using MeOH:Methyl-tert-butyl:H2O (1:3:1) for extraction and MeOH:water (1:3) for phase separation, providing an upper organic phase (used for lipid quantification) and a lower aqueous phase (used for polar and semi-polar metabolites quantification) as described in Boutet et al. (2022). Phases were separated and dried down in a SpeedVac vacuum concentrator (Thermo RVT4104). Polar and semi-polar metabolite samples, later called specialized metabolites, were resuspended in 250 µl of acetonitrile:water (1:9) containing 500 ng of Apigenin (used as internal standard) and lipid samples were resuspended in 500 µl of acetonitrile:isopropanol (7:3) (without internal standard). The parameters for liquid chromatography, mass spectrometry, and data treatment used in the untargeted lipidomic and specialized metabolites analysis are described in Boutet et al. (2022), except for the parameters modified as followed. For specialized metabolites, MZmine was run independently for leave and seed samples (Schmid et al., 2023). For lipids and specialized metabolites in leaf samples, molecular networks were generated using cosine score thresholds of 0.65 and 0.7 in negative and positive data, respectively. For specialized metabolites in seed samples, molecular networks were generated using cosine score thresholds of 0.65 and 0.75 in negative and positive data, respectively. Lipid and specialized metabolites annotation were performed in consecutive steps. First, the ESI- and ESI+ lipidomic data used for the molecular networks were searched against our library and the available MS2 spectral libraries (MassBank.NA, GNPS Public Spectral Library, NIST14 Tandem, and NIH Natural Products), with an absolute m/z tolerance of 0.02, a minimum of 4 matched peaks, and a minimal cosine score of 0.65. For the lipid analysis, the results of the database search were validated in the different clusters of the molecular network using the specific fragments and neutral losses for the different lipid classes and their MS2 spectra (Lipid Class Specific Fragments, Lipidomics Standards Initiative (LSI)). If the database search result was valid, the annotation of other features was performed by stepwise comparison from the valid lipid metabolite. Finally, Sirius software (https://bio.informatik.uni-jena.de/software/sirius/) using the CANOPUS algorithm (Kim et al., 2021) was used (Dührkop et al., 2019), in the lipid analysis for clusters of the molecular network with no

database search results and in specialized metabolites for all features. For specialized metabolites only, the annotations were futher refine to improve unclear ones, with MS2query (de Jonge et al., 2023). A minimum Tanimoto score of 0.65 was set as the threshold for accurate identification. For each feature, a confidence level score ranging from 1 to 4 were assigned as followed: 1 represents exact matches with authentic standards, 2 denotes putatively annotated compounds verified through multiple sources, 3 corresponds to compounds identified as part of putative classes, and 4 indicates uncharacterized MS/MS signals (See Data S3 and Data S4; Reisdorph et al., 2020). Lipids that showed the same annotation in positive and negative were manually removed as followed. For TAG, the accumulations in the positive file were selected. For phospholipids found in positive and negative modes, the most sensitive accumulations were selected. However, for phospholipids found in positive and negative modes, annotations containing the fatty acid composition in the negative file were used. For other lipids, the accumulations with the highest value were selected. Accumulations of lipid features were normalized according to the weight of the seeds used for extraction. Accumulations of specialized metabolite features were normalized according to the weight of the seeds and/or leaves used for extraction and the internal standard Apigenin.

Extraction and quantification of the fatty acids

Twenty mg of the same mature dry seed samples of Celine and the *flo*- mutants in control condition and under drought stress used for polar/semipolar specialized metabolites and lipid extraction was used for fatty acid quantification. Total fatty acids were measured after fatty acids methyl ester (FAME) preparation from 2 mg of material followed by gas chromatography coupled with mass spectrometry (GC-MS) analysis as previously described (Li et al., 2006).

Statistical analysis

Phenotyping data were analyzed using two factor analysis of variance (ANOVA) followed by a Tukey post hoc test for pairwise multiple comparisons using R (http://r-project.org/). Complete statistical results are presented in Table S1. For graphical representation, only significant differences between conditions (control, stress 1 and stress 2) were presented for each genotype. For statistical analysis of the specialized metabolites, only the metabolite with variation coefficient CQ > 20% were used. Metabolite data were first normalized by the median, Log transformed (base 10) and scaled by mean-centered and divided by the standard deviation of each variable using MetaboAnalyst 5.0 (https://www.metaboanalyst.ca/) (Pang et al., 2022). Principal component analysis (PCA), sparse partial least square discriminant analysis (sPLS-DA) and loadings plot presenting the discriminant features were performed using the mixOmics package in R (Rohart et al., 2017). We used the ANOVA-simultaneous component analysis (ASCA) model in MetaboAnalyst with 100 permutations to determine the impact of each factor (genotypes and conditions) and their interaction. Visual observation of the PCA and results of the ASCA that showed no significance of the interaction between both factors (specialized metabolite pvalue=0.22, lipids pvalue=0.1) lead us to compare the samples independently using the ANOVA followed by a Fisher's LSD post hoc analysis (FDR *p-value* < 0.05) in MetaboAnalyst. Upset plots were produced using the

UpSetR package (Conway et al., 2017). Hierarchical dendrograms using Ward algorithm and heat map were made in MetaboAnalyst. The cluster separations were identified using hierarchical clustering dendrograms and based on visual assessment. The integration of lipidome and specialized metabolome datasets, to explore potential associations between lipid features and specialized metabolite features, was performed using a covariance-based multiscale integration approach, operated with the sPLS-DA for two omics integration function in the mixOmics package in R (Rohart et al., 2017). From the sPLS-DA, arrow sample plots, correlation circle plot and relevance network were generated using mixOmics. For the correlation circle plot and the network analysis representations, only associations with correlation coefficient>0.55, considered moderate to strong associations (Schober and Schwarte, 2018), were used. Networks were represented using Cytoscape focusing only on lipids-metabolite correlations (Shannon et al., 2003). The enrichment analysis of the different metabolite families within significantly regulated features in control leaves and seeds were carried as in Boutet et al. (2022) and correlation analysis between flowering time, seed yield and the specialized metabolites were performed using Cytoscape (Shannon et al., 2003).

Data Availability

The lipidomic (LC-MS/MS) data on camelina seeds have been deposited at the MassiVE data repository portal with the identifier MSV000098002 (doi:10.25345/C5BZ61M9C). The untargeted metabolomic (LC-MS/MS) data on camelina seeds and leaves have been deposited at the MassiVE data repository portal with the identifier MSV000098012 (doi:10.25345/C52J68H4W).

Fundings

This work was supported by Probioraff (GENESYS PIVERT) and CAPE project (INRAE Biology and Plant breeding department). We also thank the European Union's Horizon 2020 Research and Innovation Action programme under grant agreement number 862524 (UNTWIST) for technical support. The IJPB benefits from the support of Saclay Plant Sciences-SPS (ANR-17-EUR-0007).

Acknowledgements

We thank Patrick Grillot, Michel Le Brusq and Tracy Francois for technical support and Jean-Luc Cacas for the constructive discussions on lipid annotation and interpretation. This work has benefited from the support of IJPB's Plant Observatory platform PO-Chem.

Author Contributions

JDF and AV conceptualized the research. AV, MW and MV grew the plants, conducted the drought experiment, the phenotyping and sample collections. AV and LB extracted the samples for LC–MS/MS. SB and JCT generated the LC–MS/MS data, performed the metabolite quantification and annotation. ADC extracted the fatty acid. FT carried out the fatty acid quantification and annotation. AV and MC performed the statistical analyses. AV, JDF

and MC interpreted the data. AV and JDF wrote the original draft with contribution from MC. All authors commented on and approved the submitted version.

Disclosures

Conflicts of interest: No conflicts of interest declared

References

Abrecht, D.G., Carberry, P.S., 1993. The influence of water deficit prior to tassel initiation on maize growth, development and yield. Field Crops Res 31, 55–69.

Andrés, F., Coupland, G., 2012. The genetic basis of flowering responses to seasonal cues. Nat Rev Genet 13, 627–39.

Bacelar, E., Aroca, R., 2013. Plant responses to drought stress: From morphological to molecular features. Plant Responses to Drought Stress: From Morphological to Molecular Features 1–466.

Barreda, L., Brosse, C., Boutet, S., Klewko, N., De Vos, D., Francois, T., Collet, B., Grain, D., Boulard, C., Totozafy, J.C., Bernay, B., Perreau, F., Lepiniec, L., Rajjou, L., Corso, M., 2025. Multi-omic analyses unveil contrasting composition and spatial distribution of specialized metabolites in seeds of *Camelina sativa* and other Brassicaceae. The Plant Journal 121.

Barreda, L., Brosse, C., Boutet, S., Perreau, F., Rajjou, L., Lepiniec, L., Corso, M., 2024. Specialized metabolite modifications in Brassicaceae seeds and plants: diversity, functions and related enzymes. Nat Prod Rep.

Baumert, A., Milkowski, C., Schmidt, J., Nimtz, M., Wray, V., Strack, D., 2005. Formation of a complex pattern of sinapate esters in Brassica napus seeds, catalyzed by enzymes of a serine carboxypeptidase-like acyltransferase family Phytochemistry 66, 1334–1345.

Bechtold, U., Penfold, C.A., Jenkins, D.J., Legaie, R., Moore, J.D., Lawson, T., Matthews, J.S.A., Vialet-Chabrand, S.R.M., Baxter, L., Subramaniam, S., Hickman, R., Florance, H., Sambles, C., Salmon, D.L., Feil, R., Bowden, L., Hill, C., Baker, N.R., Lunn, J.E., Finkenstädt, B., Mead, A., Buchanan-Wollaston, V., Beynon, J., Rand, D.A., Wild, D.L., Denby, K.J., Ott, S., Smirnoff, N., Mullineaux, P.M., 2016. Time-series transcriptomics reveals that AGAMOUS-LIKE22 affects primary metabolism and developmental processes in drought-stressed arabidopsis. Plant Cell 28, 345–366.

Bellec, Y., Guyon-Debast, A., François, T., Gissot, L., Biot, E., Nogué, F., Faure, J., Tepfer, M., 2022. New Flowering and Architecture Traits Mediated by Multiplex CRISPR-Cas9 Gene Editing in Hexaploid Camelina sativa. Agronomy 22.

Bennett, E., Roberts, J.A., Wagstaff, C., 2012. Manipulating resource allocation in plants. J Exp Bot. 3391–3400

Boutet, S., Barreda, L., Perreau, F., Totozafy, J.C., Mauve, C., Gakière, B., Delannoy, E., Martin-Magniette, M.L., Monti, A., Lepiniec, L., Zanetti, F., Corso, M., 2022. Untargeted metabolomic analyses reveal the diversity and plasticity of the specialized metabolome in seeds of different Camelina sativa genotypes. Plant Journal 110, 147–165.

Brock, J.R., Scott, T., Lee, A.Y., Mosyakin, S.L., Olsen, K.M., 2020. Interactions between genetics and environment shape Camelina seed oil composition. BMC Plant Biol 20.

Budin, J.T., Breene, W.M., Putnam, D.H., 1995. Some compositional properties of camelina (camelina sativa L. Crantz) seeds and oils. J Am Oil Chem Soc 72, 309–315.

Cho, L.H., Yoon, J., An, G., 2017. The control of flowering time by environmental factors. Plant Journal 90, 708–719.

Conway, J.R., Lex, A., Gehlenborg, N., 2017. UpSetR: An R package for the visualization of intersecting sets and their properties. Bioinformatics 33, 2938–2940.

Corso, M., Perreau, F., Mouille, G., Lepiniec, L., 2020. Specialized phenolic compounds in seeds: structures, functions, and regulations. Plant Science.

de Jonge, N.F., Louwen, J.J.R., Chekmeneva, E., Camuzeaux, S., Vermeir, F.J., Jansen, R.S., Huber, F., van der Hooft, J.J.J., 2023. MS2Query: reliable and scalable MS2 mass spectra-based analogue search. Nat Commun 14.

Delude, C., Fouillen, L., Bhar, P., Cardinal, M.J., Pascal, S., Santos, P., Kosma, D.K., Joubès, J., Rowland, O., Domergue, F., 2016. Primary fatty alcohols are major components of suberized root tissues of arabidopsis in the form of Alkyl hydroxycinnamates. Plant Physiol 171, 1934–1950.

Doebley, J., Stec, A., Hubbard, L., 1997. The evolution of apical dominance in maize. Nature.

Dührkop, K., Fleischauer, M., Ludwig, M., Aksenov, A.A., Melnik, A. V., Meusel, M., Dorrestein, P.C., Rousu, J., Böcker, S., 2019. SIRIUS 4: a rapid tool for turning tandem mass spectra into metabolite structure information. Nat Methods 16, 299–302.

Engels, C., Schieber, A., Gänzle, M.G., 2012. Sinapic acid derivatives in defatted Oriental mustard (Brassica juncea L.) seed meal extracts using UHPLC-DAD-ESI-MSnand identification of compounds with antibacterial activity. European Food Research and Technology 234, 535–542.

Enjalbert, J.N., Zheng, S., Johnson, J.J., Mullen, J.L., Byrne, P.F., McKay, J.K., 2013. Brassicaceae germplasm diversity for agronomic and seed quality traits under drought stress. Ind Crops Prod 47, 176–185.

Ferreira, D., Figueiredo, J., Laureano, G., Machado, A., Arrabaça, J.D., Duarte, B., Figueiredo, A., Matos, A.R., 2021. Membrane remodelling and triacylglycerol accumulation in drought stress resistance: The case study of soybean phospholipases A. Plant Physiology and Biochemistry 169, 9–21.

Franks, S.J., 2011. Plasticity and evolution in drought avoidance and escape in the annual plant Brassica rapa. New Phytologist 190, 249–257.

Franks, S.J., Sim, S., Weis, A.E., 2007. Rapid evolution of flowering time by an annual plant in response to a climate fluctuation. PNAS 104, 1278–1282.

Fukai, S., 1999. Phenology in rainfed lowland rice. Field Crops Res 64, 51–60.

Gasulla, F., Vom Dorp, K., Dombrink, I., Zähringer, U., Gisch, N., Dörmann, P., Bartels, D., 2013. The role of lipid metabolism in the acquisition of desiccation tolerance in Craterostigma plantagineum: A comparative approach. Plant Journal 75, 726–741.

Geerts, S., Raes, D., Garcia, M., Mendoza, J., Huanca, R., 2008. Crop water use indicators to quantify the flexible phenology of quinoa (Chenopodium quinoa Willd.) in response to drought stress. Field Crops Res 108, 150–156.

Gigon, A., Matos, A.R., Laffray, D., Zuily-Fodil, Y., Pham-Thi, A.T., 2004. Effect of drought stress on lipid metabolism in the leaves of Arabidopsis thaliana (Ecotype Columbia). Ann Bot 94, 345–351.

Gnan, S., Priest, A., Kover, P.X., 2014. The genetic basis of natural variation in seed size and seed number and their trade-off using Arabidopsis thaliana magic lines. Genetics 198, 1751–1758.

Gugel, R.K., Falk, K.C., 2006. Agronomic and seed quality evaluation of Camelina sativa in western Canada. Canadian Journal of Plant Science 86, 1047–1058.

Hura, T., Hura, K., Grzesiak, S., 2009. Possible contribution of cell-wall-bound ferulic acid in drought resistance and recovery in triticale seedlings. J Plant Physiol 166, 1720–1733.

Izawa, T., 2021. What is going on with the hormonal control of flowering in plants? Plant Journal 105, 431–445.

Kagale, S., Koh, C., Nixon, J., Bollina, V., Clarke, W.E., Tuteja, R., Spillane, C., Robinson, S.J., Links, M.G., Clarke, C., Higgins, E.E., Huebert, T., Sharpe, A.G., Parkin, I.A.P., 2014. The emerging biofuel crop Camelina sativa retains a highly undifferentiated hexaploid genome structure. Nat Commun 5.

Kazan, K., Lyons, R., 2016. The link between flowering time and stress tolerance. J Exp Bot 67, 47–60.

Kim, H.W., Wang, M., Leber, C.A., Nothias, L.F., Reher, R., Kang, K. Bin, Van Der Hooft, J.J.J., Dorrestein, P.C., Gerwick, W.H., Cottrell, G.W., 2021. NPClassifier: A Deep Neural Network-Based Structural Classification Tool for Natural Products. J Nat Prod.

König, S., Feussner, K., Kaever, A., Landesfeind, M., Thurow, C., Karlovsky, P., Gatz, C., Polle, A., Feussner, I., 2014. Soluble phenylpropanoids are involved in the defense response of Arabidopsis against Verticillium longisporum. New Phytologist 202, 823–837.

Leclère, M., Loyce, C., Jeuffroy, M.H., 2018. Growing camelina as a second crop in France: A participatory design approach to produce actionable knowledge. European Journal of Agronomy 101, 78–89.

Lee, S.B., Kim, H., Kim, R.J., Suh, M.C., 2014. Overexpression of Arabidopsis MYB96 confers drought resistance in Camelina sativa via cuticular wax accumulation. Plant Cell Rep 33, 1535–1546.

Li, H., Hu, X., Lovell, J.T., Grabowski, P.P., Mamidi, S., Chen, C., Amirebrahimi, M., Kahanda, I., Mumey, B., Barry, K., Kudrna, D., Schmutz, J., Lachowiec, J., Lu, C., 2021. Genetic dissection of natural variation in oilseed traits of camelina by whole-genome resequencing and QTL mapping. Plant Genome 14.

Li, Y., Beisson, F., Pollard, M., Ohlrogge, J., 2006. Oil content of Arabidopsis seeds: The influence of seed anatomy, light and plant-to-plant variation. Phytochemistry 67, 904–915.

Luo Lily, Z., Fahlgren, N., Kutchan, T., Schachtman, D., Ge, Y., Gesch, R., George, S., Dyer, J., Abdel-Haleem, H., 2021. Discovering candidate genes related to flowering time in the spring panel of Camelina sativa. Ind Crops Prod 173, 114104.

Milkowski, C., Strack, D., 2010. Sinapate esters in brassicaceous plants: Biochemistry, molecular biology, evolution and metabolic engineering. Planta. 19–35

Nadal Bigas, J., Fiers, M., van der Wal, F., Willems, L.A.J., Willemsen, V., Nijveen, H., Angenent, G.C., Immink, R.G.H., 2025. The *PEBP* genes *FLOWERING LOCUS T* and *TERMINAL FLOWER 1* modulate seed dormancy and size. J Exp Bot 76, 1049–1067.

Nakabayashi, R., Yonekura-Sakakibara, K., Urano, K., Suzuki, M., Yamada, Y., Nishizawa, T., Matsuda, F., Kojima, M., Sakakibara, H., Shinozaki, K., Michael, A.J., Tohge, T., Yamazaki, M., Saito, K., 2014. Enhancement of oxidative and drought tolerance in Arabidopsis by overaccumulation of antioxidant flavonoids. Plant Journal 77, 367–379.

Ohto, M.-A., Fischer, R.L., Goldberg, R.B., Nakamura, K., Harada, J.J., 2005. Control of seed mass by APETALA2. pnas 102, 3123–3128.

Pang, Z., Zhou, G., Ewald, J., Chang, L., Hacariz, O., Basu, N., Xia, J., 2022. Using MetaboAnalyst 5.0 for LC–HRMS spectra processing, multi-omics integration and covariate adjustment of global metabolomics data. Nat Protoc 17, 1735–1761.

Piasecka, A., Sawikowska, A., Kuczyńska, A., Ogrodowicz, P., Mikołajczak, K., Krystkowiak, K., Gudyś, K., Guzy-Wróbelska, J., Krajewski, P., Kachlicki, P., 2017. Drought-related secondary metabolites of barley (Hordeum vulgare L.) leaves and their metabolomic quantitative trait loci. Plant Journal 89, 898–913.

Praena Tamayo, J., Budzinski, I.G.F., Delhomme, N., Moritz, T., Madueño, F., Benlloch, R., 2022. Characterization of metabolic changes associated with floral transition in Arabidopsis: RAFFINOSE SYNTHASE 5 contributes to determine the timing of floral transition. bioRxiv.

Quéro, A., Molinié, R., Mathiron, D., Thiombiano, B., Fontaine, J.X., Brancourt, D., Van Wuytswinkel, O., Petit, E., Demailly, H., Mongelard, G., Pilard, S., Thomasset, B., Mesnard, F., 2016. Metabolite profiling of developing Camelina sativa seeds. Metabolomics 12, 1–14.

Rai, G.K., Kumar, P., Choudhary, S.M., Singh, H., Adab, K., Kosser, R., Magotra, I., Kumar, R.R., Singh, M., Sharma, R., Corrado, G., Rouphael, Y., 2023. Antioxidant Potential of Glutathione and Crosstalk with Phytohormones in Enhancing Abiotic Stress Tolerance in Crop Plants. Plants.

Ramirez-Prado, J.S., Latrasse, D., Rodriguez-Granados, N.Y., Huang, Y., Manza-Mianza, D., Brik-Chaouche, R., Jaouannet, M., Citerne, S., Bendahmane, A., Hirt, H., Raynaud, C., Benhamed, M., 2019. The Polycomb protein LHP1 regulates Arabidopsis thaliana stress responses through the repression of the MYC2-dependent branch of immunity. Plant Journal 100, 1118–1131.

Rathnayake, K., Parachnowitsch, A.L., 2025. Drought drives selection for earlier flowering, while pollinators drive selection for larger flowers in annual *Brassica rapa*. AoB Plants 17.

Razeq, F.M., Kosma, D.K., Rowland, O., Molina, I., 2014. Extracellular lipids of Camelina sativa: Characterization of chloroform-extractable waxes from aerial and subterranean surfaces. Phytochemistry 106, 188–196.

Raziei, Z., Kahrizi, D., Rostami-Ahmadvandi, H., 2018. Effects of climate on fatty acid profile in *Camelina sativa*. Cell Mol Biol 64, 91–96.

Reisdorph, N.A., Walmsley, S., Reisdorph, R., 2020. A perspective and framework for developing sample type specific databases for LC/MS-based clinical metabolomics. Metabolites 10.

Riboni, M., Galbiati, M., Tonelli, C., Conti, L., 2013. GIGANTEA enables drought escape response via abscisic acid-dependent activation of the florigens and SUPPRESSOR of OVEREXPRESSION of CONSTANS. Plant Physiol 162, 1706–1719.

Rohart, F., Gautier, B., Singh, A., Lê Cao, K.A., 2017. mixOmics: An R package for 'omics feature selection and multiple data integration. PLoS Comput Biol 13.

Schmid, R., Heuckeroth, S., Korf, A., Smirnov, A., Myers, O., Dyrlund, T.S., Bushuiev, R., Murray, K.J., Hoffmann, N., Lu, M., Sarvepalli, A., Zhang, Z., Fleischauer, M., Dührkop, K., Wesner, M., Hoogstra, S.J., Rudt, E., Mokshyna, O., Brungs, C., Ponomarov, K., Mutabdžija, L., Damiani, T., Pudney, C.J., Earll, M., Helmer, P.O., Fallon, T.R., Schulze, T., Rivas-Ubach, A., Bilbao, A., Richter, H., Nothias, L.-F., Wang, M., Orešič, M., Weng, J.-K., Böcker, S., Jeibmann, A., Hayen, H., Karst, U., Dorrestein, P.C., Petras, D., Du, X., Pluskal, T., 2023. Integrative analysis of multimodal mass spectrometry data in MZmine 3. Nat Biotechnol 41, 447–449.

Shannon, P., Markiel, A., Ozier, O., Baliga, N.S., Wang, J.T., Ramage, D., Amin, N., Schwikowski, B., Ideker, T., 2003. Cytoscape: A software Environment for integrated models of biomolecular interaction networks. Genome Res 13, 2498–2504.

Shavrukov, Y., Kurishbayev, A., Jatayev, S., Shvidchenko, V., Zotova, L., Koekemoer, F., De Groot, S., Soole, K., Langridge, P., 2017. Early flowering as a drought escape mechanism in plants: How can it aid wheat production? Front Plant Sci 8, 1–8.

Shoesmith, J.R., Solomon, C.U., Yang5, X., Wilkinson, L.G., Sheldrick, S., Eijden, E. Van, Couwenberg, S., Pugh, L.M., Eskan, M., Stephens, J., Barakate, A., Drea, S., Houston, K., Tucker, M.R., McKim, S.M., 2021. APETALA2 functions as a temporal factor together with BLADE-ON-PETIOLE2 and MADS29 to control flower and grain development in barley. Development (Cambridge) 148.

Soppe, W.J.J., Viñegra de la Torre, N., Albani, M.C., 2021. The Diverse Roles of FLOWERING LOCUS C in Annual and Perennial Brassicaceae Species. Front Plant Sci.

Soviguidi, D.R.J., Pan, R., Liu, Y., Rao, L., Zhang, W., Yang, X., 2022. Chlorogenic acid metabolism: The evolution and roles in plant response to abiotic stress. Phyton-International Journal of Experimental Botany.

tesaki, s, Tanabe, S., Ono, H., Fukushi, E., Kawabata, J., Watanabe, M., 1998. 4-Hydroxy-3-nitrophenylacetic and Sinapic Acids as Antibacterial Compounds from Mustard Seeds. Biosci. Biotechnolo. Biochem. 998–1000.

Torres-Franklin, M.L., Gigon, A., De Melo, D.F., Zuily-Fodil, Y., Pham-Thi, A.T., 2007. Drought stress and rehydration affect the balance between MGDG and DGDG synthesis in cowpea leaves. Physiol Plant 131, 201–210.

Upchurch, RG., 2008. atty acid unsaturation, mobilization, and regulation in the response of plants to stress. Biotechnol Letter 967–977.

Van Daele, I., Gonzalez, N., Vercauteren, I., de Smet, L., Inzé, D., Roldán-Ruiz, I., Vuylsteke, M., 2012. A comparative study of seed yield parameters in Arabidopsis thaliana mutants and transgenics. Plant Biotechnol J 10, 488–500.

Vishwanath, S.J., Kosma, D.K., Pulsifer, I.P., Scandola, S., Pascal, S., Joubès, J., Dittrich-Domergue, F., Lessire, R., Rowland, O., Domergue, F., 2013. Suberin-associated fatty alcohols in Arabidopsis: Distributions in roots and contributions to seed coat barrier properties. Plant Physiol 163, 1118–1132.

Vollmann, J., Moritz, T., Kargl, C., Baumgartner, S., Wagentristl, H., 2007. Agronomic evaluation of camelina genotypes selected for seed quality characteristics. Ind Crops Prod 26, 270–277.

Wahl, V., Ponnu, J., Schlereth, A., Arrivault, S., Langenecker, T., Franke, A., Feil, R., Lunn, J.E., Stitt, M., Schmid, M., 2013. Regulation of Flowering by Trehalose-6-Phosphate Signaling in Arabidopsis thaliana. Science (1979) 704–708.

Wang, Z., Wang, F., Hong, Y., Yao, J., Ren, Z., Shi, H., Zhu, J.K., 2018. The Flowering Repressor SVP Confers Drought Resistance in Arabidopsis by Regulating Abscisic Acid Catabolism. Mol Plant 11, 1184–1197.

Zanetti, F., Alberghini, B., Marjanović Jeromela, A., Grahovac, N., Rajković, D., Kiprovski, B., Monti, A., 2021. Camelina, an ancient oilseed crop actively contributing to the rural renaissance in Europe. A review. Agron Sustain Dev 41.

Zanetti, F., Eynck, C., Christou, M., Krzyżaniak, M., Righini, D., Alexopoulou, E., Stolarski, M.J., Van Loo, E.N., Puttick, D., Monti, A., 2017. Agronomic performance and seed quality attributes of Camelina (Camelina sativa L. crantz) in multi-environment trials across Europe and Canada. Ind Crops Prod 107, 602–608.

Zeiss, D.R., Piater, L.A., Dubery, I.A., 2021. Hydroxycinnamate Amides: Intriguing Conjugates of Plant Protective Metabolites. Trends Plant Sci.

Zhang, B., Li, C., Li, Y., Yu, H., 2020. Mobile TERMINAL FLOWER1 determines seed size in Arabidopsis. Nat Plants 6, 1146–1157.

Figure legends:

Figure 1: Drought impacts strongly the *flo*- branching phenotype but slightly the flowering precocity

A, Picture of the wt and the *B1-2*, *C2-19, A40-24*, *B23-3*, *A4-12* and *A1-14* mutants in the control condition (top) and 4 days after the end of the 10-day drought stress (bottom; day 34). Arrows indicate the absence of lateral branches in the *A1-14* and *A4-12* mutants. Bar, 15-cm. B, Days to flowering (days to the first flower open) of the wt and the *B1-2*, *C2-19, A40-24*, *B23-3*, *A4-12* and *A1-14* mutants in the control and in response to drought (stress 1). C, Branch number of the wt and the *B1-2*, *C2-19, A40-24*, *B23-3*, *A4-12* and *A1-14* mutants observed at the end of the 10-day drought stress (day 30) in the control and in response to drought (stress 1). In B and C, boxes indicate the interquartile range, the vertical line in the middle is the median, the horizontal lines (whiskers)

correspond to the highest or lowest value within 1.5 times the interquartile range, letters show significant differences between conditions and genotypes ($p<0.05$, using ANOVA followed by Tukey's pairwise multiple comparisons), *n* = 10 to 12

Figure 2: Drought before and after flowering impacts final plant size and yield

A-C, Final plant lenght (A), seed yield (B) and thousand seeds weight (C) of wt and the *B1-2*, *C2-19, A40-24*, *B23-3*, *A4-12* and *A1-14* plants in control condition and in response to early drought (stress 1) and drought at flowering (stress 2). Boxes indicate the interquartile range, the vertical line in the middle is the median, the horizontal lines (whiskers) correspond to the highest or lowest value within 1.5 times the interquartile range, letters show significant differences between conditions only ($p<0.05$, using ANOVA followed by Tukey's pairwise multiple comparisons; additional pairwise comparisons between genotypes are available in Table S1), *n* = 10 to 12.

Figure 3: Seed lipidome showed only few metabolic changes after drought stress in wild type camelina

A, Principal component analysis (PCA) showing the positions of samples in the plane delineated by component 1 and 2 accounting for 43% of the total variance between the 178 features identified as accumulated in mature seeds of the wt and the *flo*- mutants (*A1-14*, *A4-12*, *A40-24*, *B1-2*, *B23-3* and *C2-19*) in control condition (triangles) and in response to stress 2 (circles). B, UpSet plot showing the number of features differentially accumulated in the control condition compared to stress 2 (*P-values* after ANOVA and Fisher's FDR correction lower than 0.05) for each of the genotype, wt and the *flo*- mutants (bottom left hand side) and the number of unique and shared differentially accumulated features (right-hand side). This UpSet plot represents 61% of the total differential features. The grey box shows the intersections that account for 50% of the 79 significantly regulated features across genotypes and conditions. The plot on the right-hand side shows the number of features with differential accumulation under drought specific to a single genotype (indicated by a black circle alone) and those with shared differential accumulation across genotypes (indicated by black circles connected by a line). For example, the most frequent combination corresponded to features differentially accumulated upon drought only in the wt, followed by features showing shared differential accumulation under stress in *B23-3* and *A4-12*. C, Heat map representing the hierarchical clustering of the 79 features significantly regulated features in at least one of the pairwise comparison. Stars shows significant difference between wt control *vs* wt stress 2 with *P-values* after ANOVA and Fisher's FDR correction lower than 0.05. D, Box plots of the normalized accumulation profile of features of cluster 1A, 1B, 2A and 2B. In B and C the black stars indicate the 16 features significantly regulated in the wt in response to stress 2, the red star the features highly accumulated in response to stress 2 in all *flo*- mutant but not in the wt.

Figure 4: The *flo*- mutants showed a different specialized metabolome response to drought stress in mature seeds compared to the wt

A, Principal component analysis (PCA) showing the positions of samples in the plane delineated by component 1 and 2 accounting for 41% of the total variance between the 1761 features identified accumulated in mature

seeds of the wt and the *flo*- mutants (*A1-14*, *A4-14*, *A40-24*, *B1-2*, *B23-3* and *C2-19*) in control condition (triangles) and in response to stress 2 (circles). B, UpSet plot showing the number of features differentially accumulated in the control condition compared to stress 2 (*P-values* after ANOVA and Fisher's FDR correction lower than 0.05) for each of the genotype, wt and the *flo*- mutants (bottom left hand side) and the number of unique and shared differentially accumulated features (right-hand side). This UpSet plot represents 59% of the total differential features. The grey box shows the intersections that account for 50% of the 1277 significantly regulated features across genotypes and conditions. The plot on the right-hand side shows the number of features with differential accumulation under drought specific to a single genotype (indicated by a black circle alone) and those with shared differential accumulation across genotypes (indicated by black circles connected by a line). For example, eleven features were identified as differentially accumulated under drought in all *flo*- mutants, but not in the wt. C, Heatmap representing the hierarchical clustering of the 202 features significantly regulated in mature seeds of the wt in response to stress 2 in all genotypes (wt, *A1-14*, *A4-14*, *A40-24*, *B1-2*, *B23-3* and *C2-19*). Coexpressed clusters were assigned into two higher level clusters (1 and 2). D and F, box plot of the normalized accumulation profile of features of cluster 1 (D) and cluster 2A (F). E and G, Structure of the annotated features of cluster 1 (E) and cluster 2A (G).

Figure 5: Integration of specialized metabolite and lipid features identified correlations between hydroxycinnamic acids and alkyl hydroxycinnamates

A, Arrow sample plot, from the sPLS-DA applied to the lipid and specialized metabolite datasets showing how each sample project in both. The start and the end of the arrow indicates the sample projection on the two components from the lipids to the specialized metabolites data respectivly. While strong differences between genotypes in both datasets is observed in dimension 1, the long arrows in all genotypes indicate low agreement at the sample level. B, Network analysis applied to the lipid and specialized metabolite datasets. Each edge links a specialized metabolite (square) to a lipid (circle). Only variables selected in the sPLS-DA on the first two components are represented and filtered with a cutoff of 0.55. Only clusters with pairs of variables belonging to different omics are presented. Red: positive correlations, blue: negative correlations. C-D, Structures of the annotated lipid features (C) and specialized metabolites (D) of the network presented on the right in B. In C, the location of double bonds in the lipid structures are putatives.

Figure 6: The *A4-12* and *A1-14 flo*- mutants show strong modifications of specialized metabolomes in seeds and leaves

A, sPLS-DA showing model discrimination between seed samples of the wt and the *A1-14*, *A4-14*, *A40-24*, *B1-2*, *B23-3* and *C2-19 flo*- mutants. sPLS-DA allows the selection of the most predictive or discriminative features within the dataset to classify samples. B, Molecule structures of the annotated putative metabolites in the 20 most discriminating features of component 1 of A. C, sPLS-DA showing model discrimination between leaf samples of the wt and the *A1-14*, *A4-14*, *A40-24*, *B1-2*, *B23-3* and *C2-19 flo*- mutants. D, Molecule structures of the annotated putative metabolites in the 20 most discriminating features of component 1 of C. The start

871 indicates that palmitamide (p139) was also identified differentially accumulated in response to drought in the wt
872 (Figure 4E).
873
874 **Figure 7:** Specialized metabolites correlated with flowering time and yield
875 A-C, Principal component analysis (PCA) showing the positions of lipids (A) and specialized metabolites (B and C)
876 samples in the plane delineated by component 1 and 2 in mature seeds (A and B) and in leaves (C) of the wt
877 (Celine), the *flo*- mutants (*B1-2*, *C2-19, A40-24*, *B23-3*, *A4-12* and *A1-14*), and the CAM221, L2F4, CN101981,
878 CAM151 and CAM203 additional genotypes. *n* = 3. D and F, Correlation networks of specialized metabolites in
879 mature seeds (D) and leaves (F), FT: Flowering Time, Y: seed Yield, red line: positive correlation > 0.8, blue line:
880 negative correlation < -0.8. E, Molecule structures of the annotated putative metabolites in D.

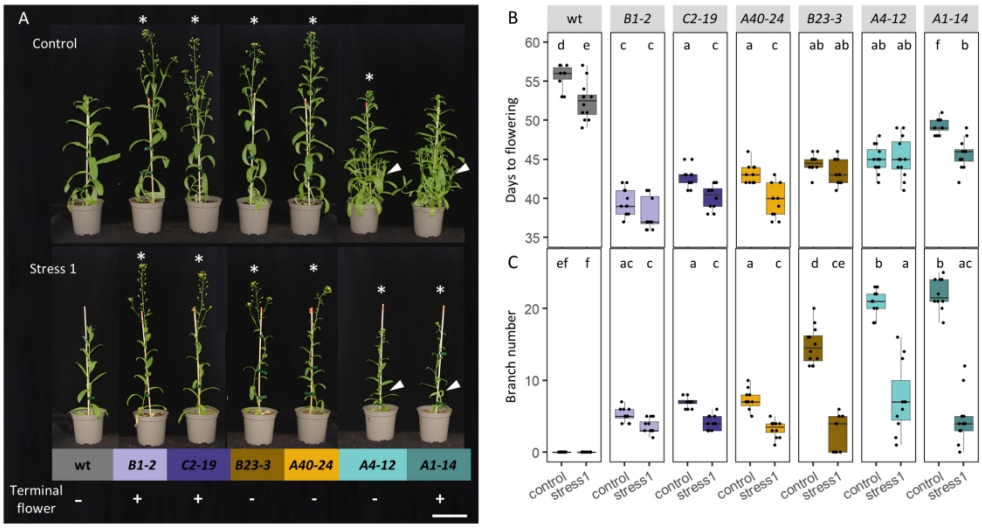

Figure 1: Drought impacts strongly the *flo*- branching phenotype but slightly the flowering precocity. A, Picture of the wt and the *B1-2*, *C2-19*, *A40-24*, *B23-3*, *A4-12* and *A1-14* mutants in the control condition (top) and 4 days after the end of the 10-day drought stress (bottom; day 34). Arrows indicate the absence of lateral branches in the *A1-14* and *A4-12* mutants. Bar, 15-cm. B, Days to flowering (days to the first flower open) of the wt and the *B1-2*, *C2-19*, *A40-24*, *B23-3*, *A4-12* and *A1-14* mutants in the control and in response to drought (stress 1). C, Branch number of the wt and the *B1-2*, *C2-19*, *A40-24*, *B23-3*, *A4-12* and *A1-14* mutants observed at the end of the 10-day drought stress (day 30) in the control and in response to drought (stress 1). In B and C, boxes indicate the interquartile range, the vertical line in the middle is the median, the horizontal lines (whiskers) correspond to the highest or lowest value within 1.5 times the interquartile range, letters show significant differences between conditions and genotypes ($p<0.05$, using ANOVA followed by Tukey's pairwise multiple comparisons), n = 10 to 12

188x100mm (300 x 300 DPI)

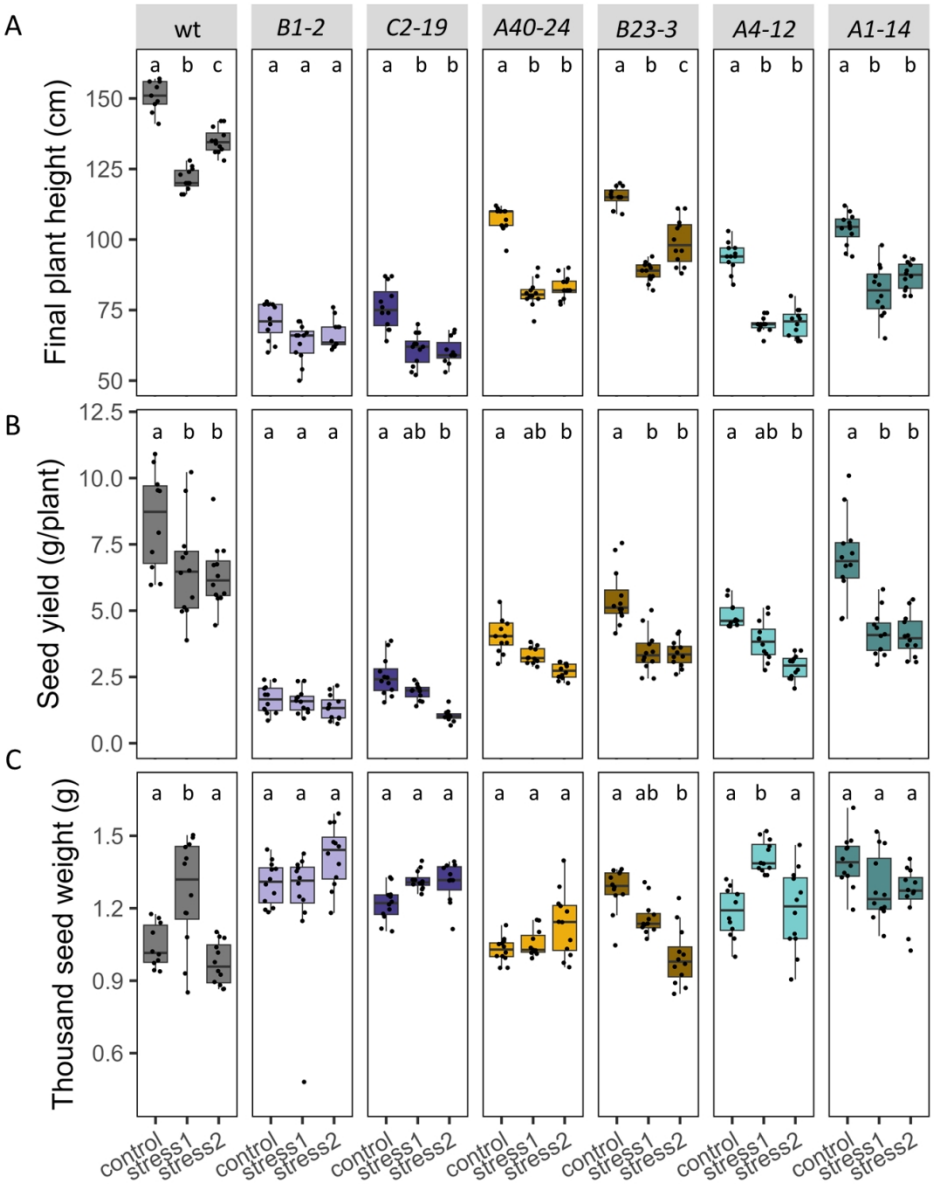

Figure 2: Drought before and after flowering impacts final plant size and yield. A-C, Final plant lenght (A), seed yield (B) and thousand seeds weight (C) of wt and the *B1-2*, *C2-19*, *A40-24*, *B23-3*, *A4-12* and *A1-14* plants in control condition and in response to early drought (stress 1) and drought at flowering (stress 2). Boxes indicate the interquartile range, the vertical line in the middle is the median, the horizontal lines (whiskers) correspond to the highest or lowest value within 1.5 times the interquartile range, letters show significant differences between conditions only ($p<0.05$, using ANOVA followed by Tukey's pairwise multiple comparisons; additional pairwise comparisons between genotypes are available in Table S1), n = 10 to 12.

114x142mm (300 x 300 DPI)

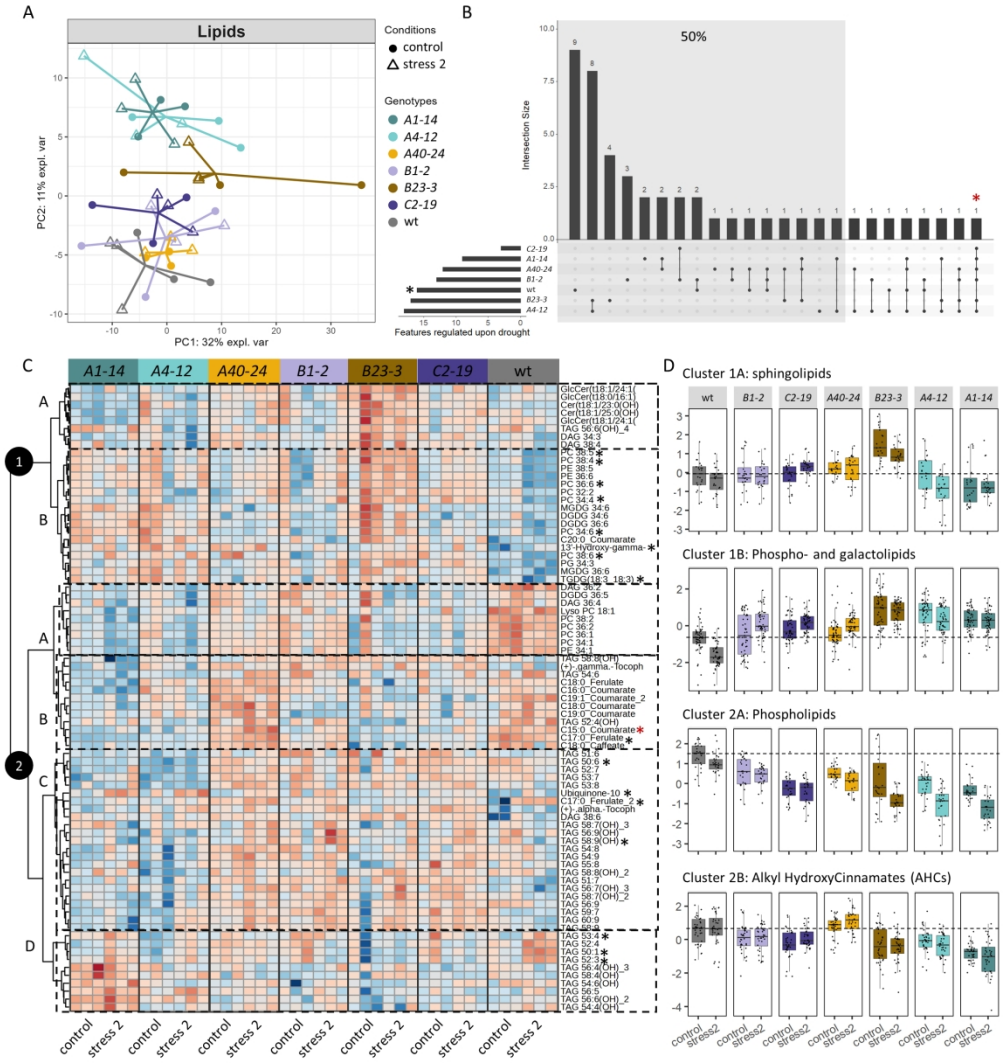

Figure 3: Seed lipidome showed only few metabolic changes after drought stress in wild type camelina. A, Principal component analysis (PCA) showing the positions of samples in the plane delineated by component 1 and 2 accounting for 43% of the total variance between the 178 features identified as accumulated in mature seeds of the wt and the *flo*- mutants (*A1-14*, *A4-12*, *A40-24*, *B1-2*, *B23-3* and *C2-19*) in control condition (triangles) and in response to stress 2 (circles). B, UpSet plot showing the number of features differentially accumulated in the control condition compared to stress 2 (*P-values* after ANOVA and Fisher's FDR correction lower than 0.05) for each of the genotype, wt and the *flo*- mutants (bottom left hand side) and the number of unique and shared differentially accumulated features (right-hand side). This UpSet plot represents 61% of the total differential features. The grey box shows the intersections that account for 50% of the 79 significantly regulated features across genotypes and conditions. The plot on the right-hand side shows the number of features with differential accumulation under drought specific to a single genotype (indicated by a black circle alone) and those with shared differential accumulation across genotypes (indicated by black circles connected by a line). For example, the most frequent combination corresponded to features differentially accumulated upon drought only in the wt, followed by features showing shared differential accumulation under stress in *B23-3* and *A4-12*. C, Heat map representing the hierarchical clustering of the 79 features significantly regulated features in at least one of the pairwise comparison. Stars shows significant difference between wt control vs wt stress 2 with *P-values* after ANOVA and Fisher's FDR correction lower than 0.05. D, Box plots of the normalized accumulation profile of features of cluster 1A, 1B,

2A and 2B. In B and C the black stars indicate the 16 features significantly regulated in the wt in response to stress 2, the red star the features highly accumulated in response to stress 2 in all flo- mutant but not in the wt.

187x203mm (300 x 300 DPI)

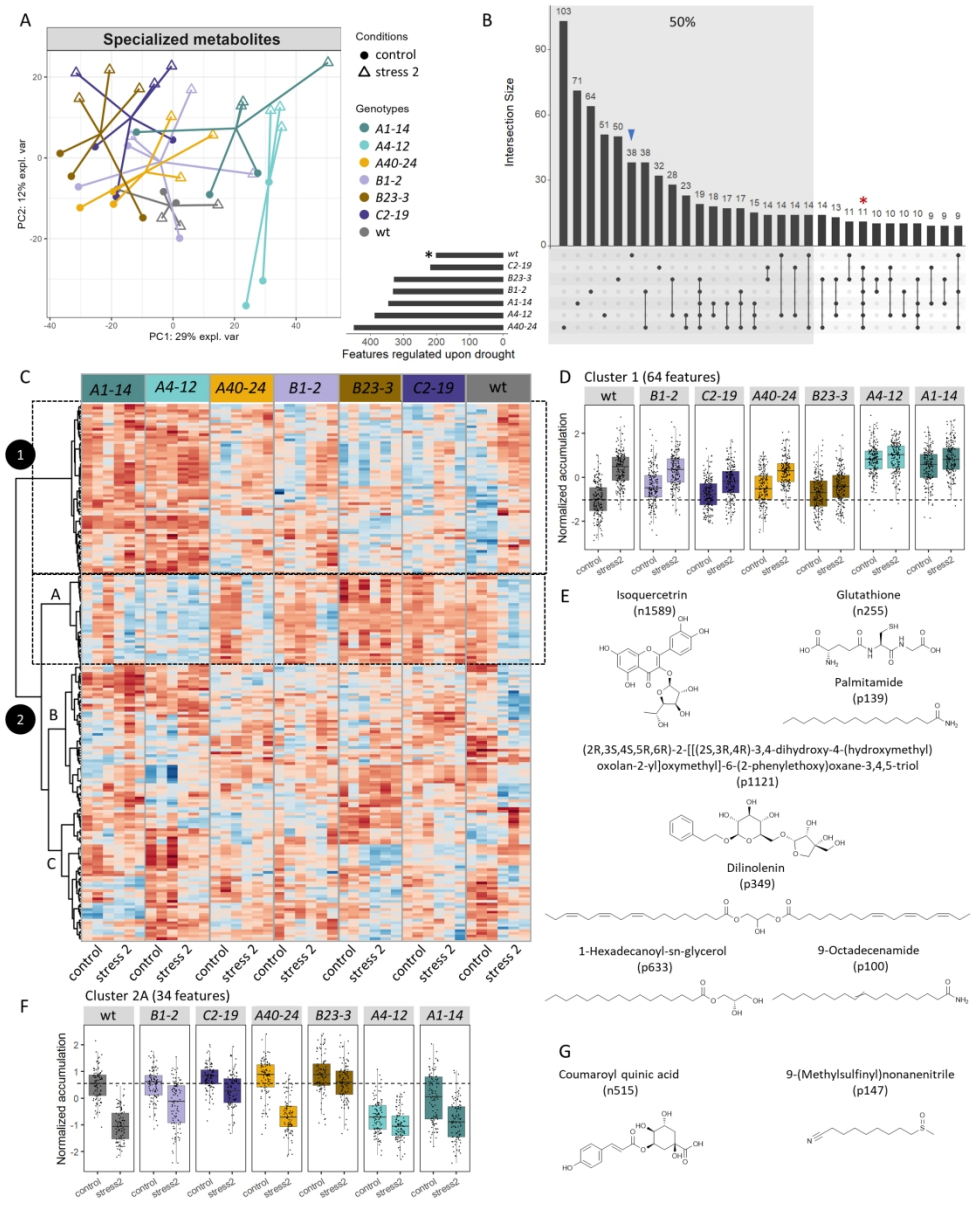

Figure 4: The *flo*- mutants showed a different specialized metabolome response to drought stress in mature seeds compared to the wt. A, Principal component analysis (PCA) showing the positions of samples in the plane delineated by component 1 and 2 accounting for 41% of the total variance between the 1761 features identified accumulated in mature seeds of the wt and the *flo*- mutants *A1-14*, *A4-12*, *A40-24*, *B1-2*, *B23-3* and *C2-19*) in control condition (triangles) and in response to stress 2 (circles). B, UpSet plot showing the number of features differentially accumulated in the control condition compared to stress 2 (*P-values* after ANOVA and Fisher's FDR correction lower than 0.05) for each of the genotype, wt and the *flo*- mutants (bottom left hand side) and the number of unique and shared differentially accumulated features (right-hand side). This UpSet plot represents 59% of the total differential features. The grey box shows the intersections that account for 50% of the 1277 significantly regulated features across genotypes and conditions. The plot on the right-hand side shows the number of features with differential accumulation under drought specific to a single genotype (indicated by a black circle alone) and those with shared differential accumulation across genotypes (indicated by black circles connected by a line). For example, eleven features were identified as differentially accumulated under drought in all *flo*- mutants, but not in the wt. C, Heatmap representing the

hierarchical clustering of the 202 features significantly regulated in mature seeds of the wt in response to stress 2 in all genotypes (wt, *A1-14*, *A4-12*, *A40-24*, *B1-2*, *B23-3* and *C2-19*). Coexpressed clusters were assigned into two higher level clusters (1 and 2). D and F, box plot of the normalized accumulation profile of features of cluster 1 (D) and cluster 2A (F). E and G, Structure of the annotated features of cluster 1 (E) and cluster 2A (G).

181x221mm (300 x 300 DPI)

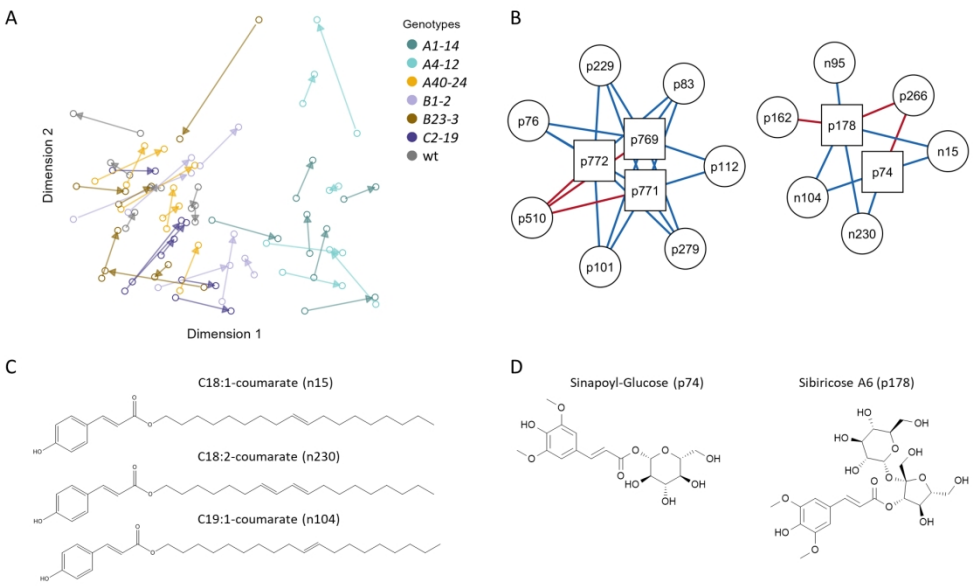

Figure 5: Integration of specialized metabolite and lipid features identified correlations between hydroxycinnamic acids and alkyl hydroxycinnamates

A, Arrow sample plot, from the sPLS-DA applied to the lipid and specialized metabolite datasets showing how each sample project in both. The start and the end of the arrow indicates the sample projection on the two components from the lipids to the specialized metabolites data respectivly. While strong differences between genotypes in both datasets is observed in dimension 1, the long arrows in all genotypes indicate low agreement at the sample level. B, Network analysis applied to the lipid and specialized metabolite datasets. Each edge links a specialized metabolite (square) to a lipid (circle). Only variables selected in the sPLS-DA on the first two components are represented and filtered with a cutoff of 0.55. Only clusters with pairs of variables belonging to different omics are presented. Red: positive correlations, blue: negative correlations. C-D, Structures of the annotated lipid features (C) and specialized metabolites (D) of the network presented on the right in B. In C, the location of double bonds in the lipid structures are putatives.

172x102mm (300 x 300 DPI)

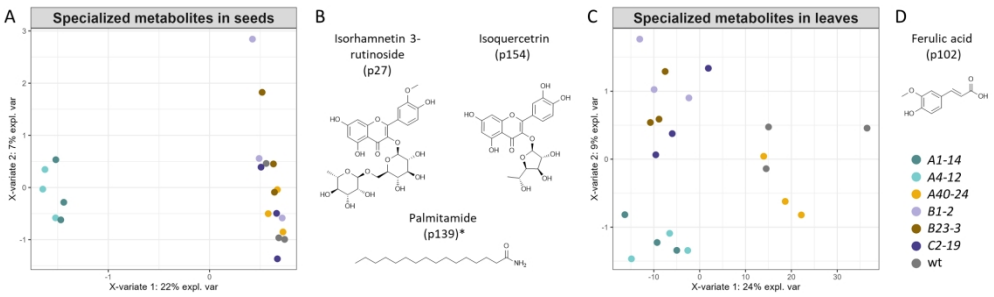

Figure 6: The *A4-12* and *A1-14 flo-* mutants show strong modifications of specialized metabolomes in seeds and leaves A, sPLS-DA showing model discrimination between seed samples of the wt and the *A1-14*, *A4-14*, *A40-24*, *B1-2*, *B23-3* and *C2-19 flo-* mutants. sPLS-DA allows the selection of the most predictive or discriminative features within the dataset to classify samples. B, Molecule structures of the annotated putative metabolites in the 20 most discriminating features of component 1 of A. C, sPLS-DA showing model discrimination between leaf samples of the wt and the *A1-14*, *A4-14*, *A40-24*, *B1-2*, *B23-3* and *C2-19 flo-* mutants. D, Molecule structures of the annotated putative metabolites in the 20 most discriminating features of component 1 of C. The start indicates that palmitamide (p139) was also identified differentially accumulated in response to drought in the wt (Figure 4E).

186x55mm (300 x 300 DPI)

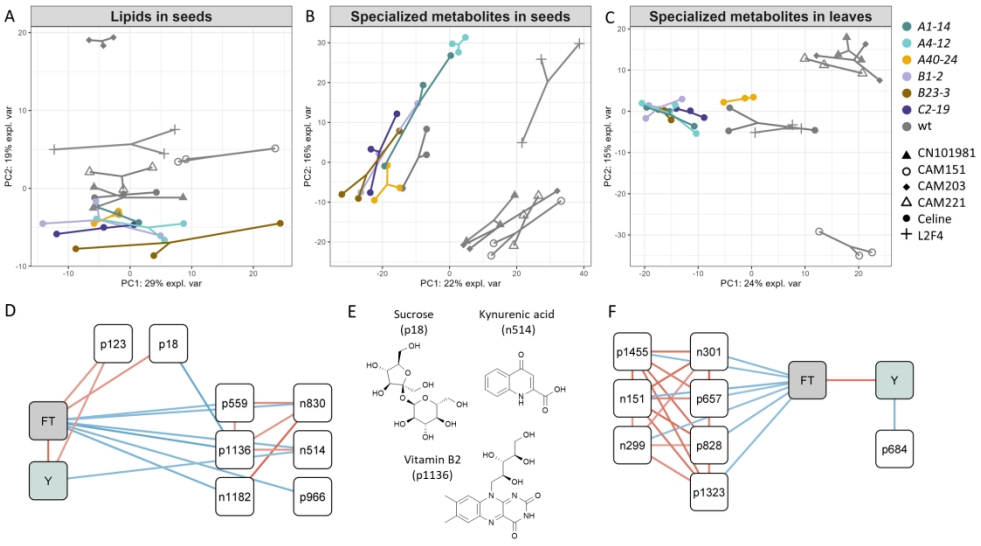

Figure 7: Specialized metabolites correlated with flowering time and yield.
A-C, Principal component analysis (PCA) showing the positions of lipids (A) and specialized metabolites (B and C) samples in the plane delineated by component 1 and 2 in mature seeds (A and B) and in leaves (C) of the wt (Celine), the *flo*- mutants (*B1-2*, *C2-19*, *A40-24*, *B23-3*, *A4-12* and *A1-14*), and the CAM221, L2F4, CN101981, CAM151 and CAM203 additional genotypes. *n* = 3. D and F, Correlation networks of specialized metabolites in mature seeds (D) and leaves (F), FT: Flowering Time, Y: seed Yield, red line: positive correlation > 0.8, blue line: negative correlation < -0.8. E, Molecule structures of the annotated putative metabolites in D.

192x104mm (300 x 300 DPI)

	SVP			*FLC*			*LHP1*			*TFL1*			*ELF3*		
	SG-1 Csa16g 044290	*SG-2 Csa07g 052630*	*SG-3 Csa09g 086860*	*SG-1 Csa13g 011890*	*SG-2 Csa08g 054450*	*SG-3 Csa20g 015400*	*SG-1 Csa13g 020480*	*SG-2 Csa08g 009910*	*SG-3 Csa20g 025860*	*SG-1 Csa13g 003940*	*SG-2 Csa08g 060650*	*SG-3 Csa20g0 05030*	*SG-1 Csa16g 047550*	*SG-2 Csa07 g0569 50*	*SG-3 Csa09g 092140*
A40-24	WT WT	WT WT	WT +C	WT WT	WT +T	WT WT	-20 WT	WT WT	WT WT	+T +A	WT WT	+G WT	WT WT	WT WT	WT WT
A4-12	WT WT	WT WT	WT WT	WT WT	WT WT	WT WT	+C -ACG	WT -4	WT WT	+T WT/-2	WT +A	WT -4 & 2snp	WT WT	WT WT	WT WT
A1-14	WT WT	WT +C	WT WT	WT WT	WT WT	WT WT	WT 5	WT -4	-123 -123	+A WT	WT +A	WT WT	WT WT	WT WT	WT WT
B23-3	WT WT	WT WT	WT -34	WT WT	WT WT	WT WT	WT +A	+A WT	WT -A	WT WT	+A WT	WT WT	WT WT	WT WT	WT WT
B1-2	WT +T	WT +C	WT -5	WT WT	WT WT	WT WT	+A WT	+A -10/snp	+C WT	+A +C	+T -4	WT -4	-T & snp WT	WT WT	WT WT
C2-19	WT -41	WT WT	WT -4	WT WT	WT WT	WT WT	+C WT/-1	+A +T	-G WT	+T +T	+C -4	Complex deletions	-C WT	WT WT	WT WT

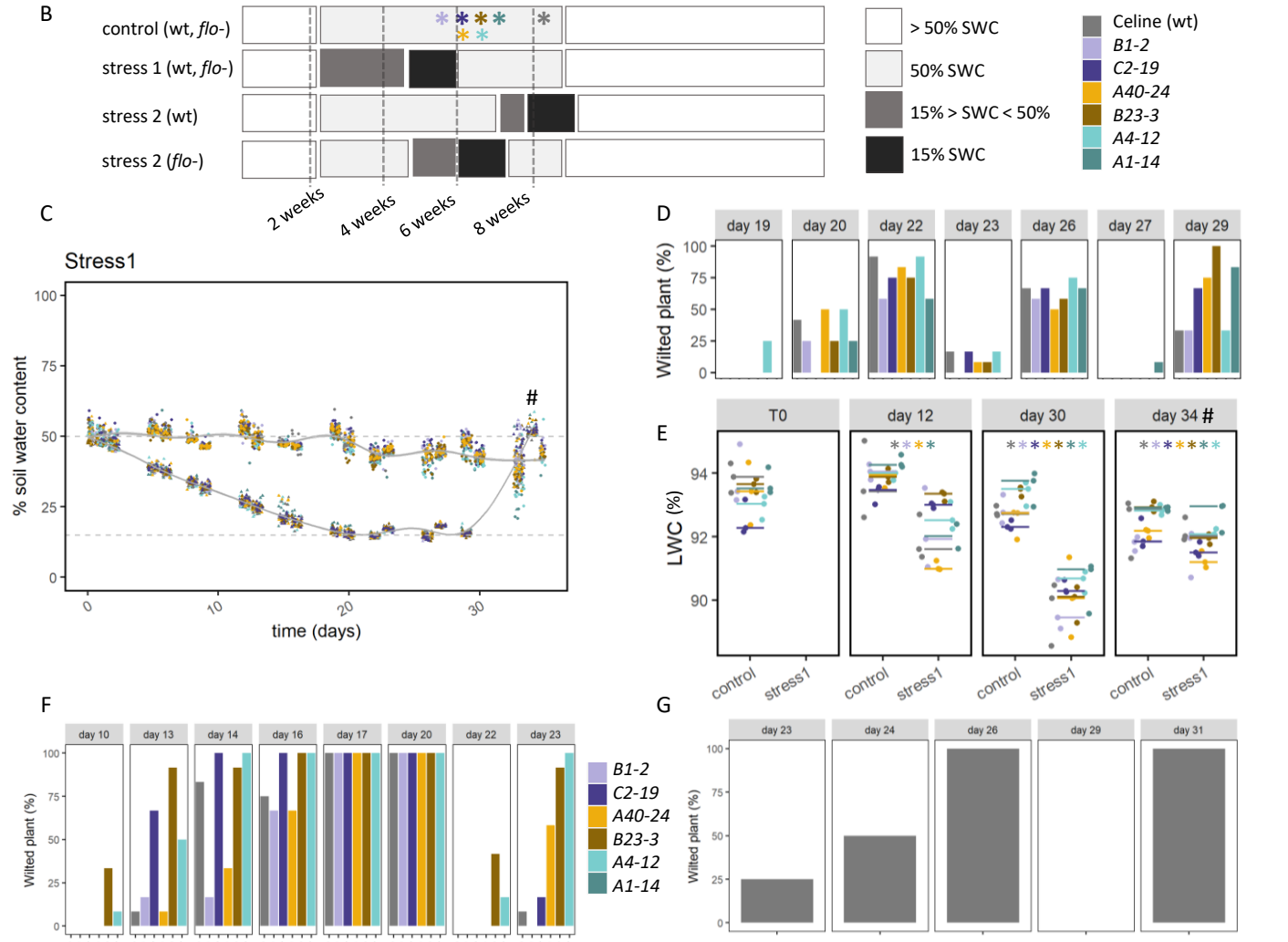

Figure S1: *flo-* mutant genotypes and parameters of the two drought stresses.

A, Genotypes of the *B1-2*, *C2-19, A40-24*, *B23-3*, *A4-12* and *A1-14 flo-* mutants at the three homeologs of *SVP*, *FLC*, *LHP1*, *TFL1* and *ELF3* as described in Bellec et al., 2022. In each cell, sequenced alleles are presented for the two sgRNAs positions: wild-type (WT) or the indicated mutation; insertions or deletions (− or + nucleotides), single nucleotide polymorphism (snp), and complex deletions. All yellow boxes indicate homozygous mutations in at least one of the sgRNAs position. Light yellow boxes stipulate alleles with no modification of frameshift. B, Diagram representation of the experimental design of the two drought stresses carried before flowering (stress 1) and on flowering plants (stress 2) carried out on the wt and the *B1-2*, *C2-19, A40-24*, *B23-3*, *A4-12* and *A1-14 flo-* mutants. Stress 2 started on 6 week-old plants for the *flo-* mutants and 8 week-old plants for the wt plants. The black boxes represent the 10-day stress period at 15% soil water content (SWC), the dark grey boxes the water loss between 50% to 15% SWC, the light grey boxes indicate the period when plants were maintained at 50% SWC and the empty boxes, the period when plant were watered in excess (>50% SWC). Stars indicate the mean day to flowering of the different genotypes. C, Percentage of soil water content (SWC) of the control and stress 1 plants. Day 0 indicates the beginning of the loss from 50% to 15% SWC. D, Percentage of wilted plant during the 10-day of stress 1 (day 19 to day 29) in the wt and the *flo-* mutants. E, Percentage of Leaf Water Content (LWC) at day 0 (T0), day 12 day 30 and day 34 of stress 1 carried out on leaf 2, 4, 9 and 12 respectively. Lines indicate the median. Stars show significant differences between control and stress 1 ($p<0.05$, using ANOVA followed by Tukey's pairwise multiple comparisons), $n = 3$. F-G, Percentage of wilted plant during the stress 2 in the *flo-* mutant plants (F; day 10 to day 33) and in the wt plants (G; day 23 to day 31). In C and E, # indicate the recovery time point. $n = 10$ to 12

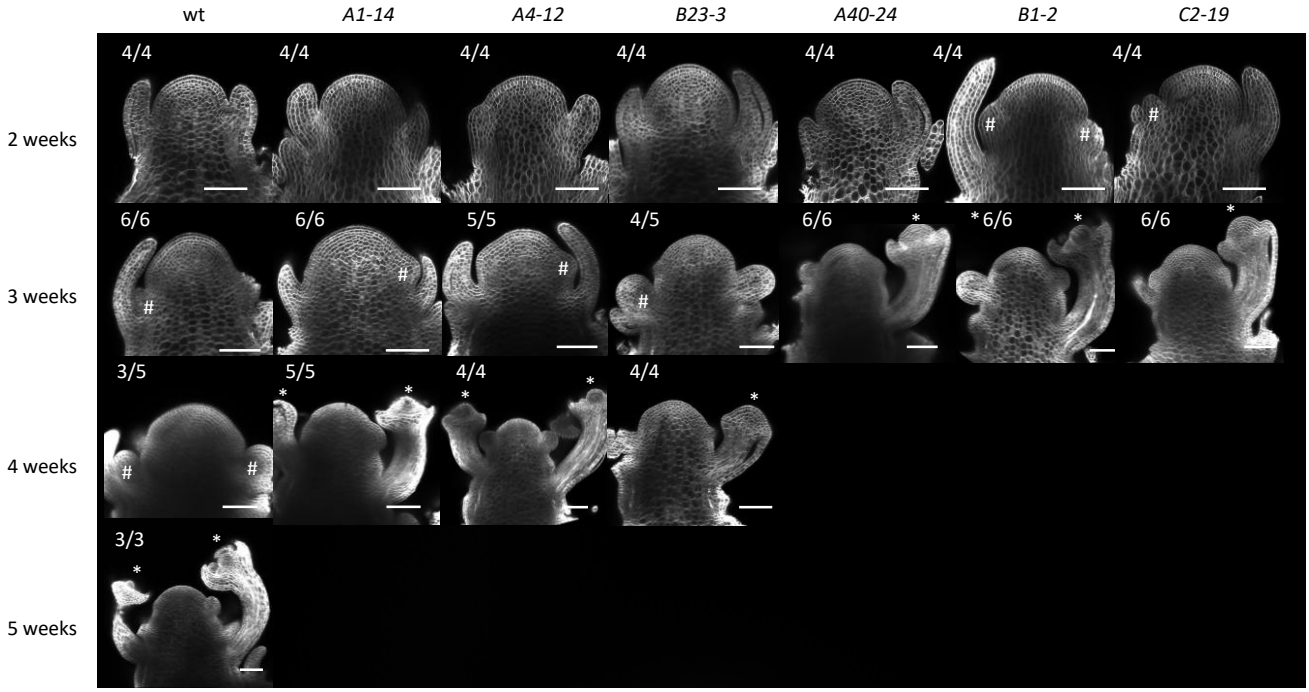

Figure S2: Morphology of the shoot apical meristem of the wt and the *B1-2*, *C2-19, A40-24*, *B23-3*, *A4-12* and *A1-14 flo*- mutants.

Confocal microscopy images of transversal view of the shoot apical meristem of the wt and the *B1-2*, *C2-19, A40-24*, *B23-3*, *A4-12* and *A1-14 flo*- mutants grown under 2, 3, 4 and 5 weeks in long-day conditions. Arrows indicate the presence of leaf primordia. Stars indicate flower in development present on the side of the shoot apical meristem. Hashtags indicate putative axillary meristem in the cauline leaf primordia axis. Ratio in the top left of the images indicate the number of shoot apical meristem observed with this morphology. Scale bar, 100 µm.

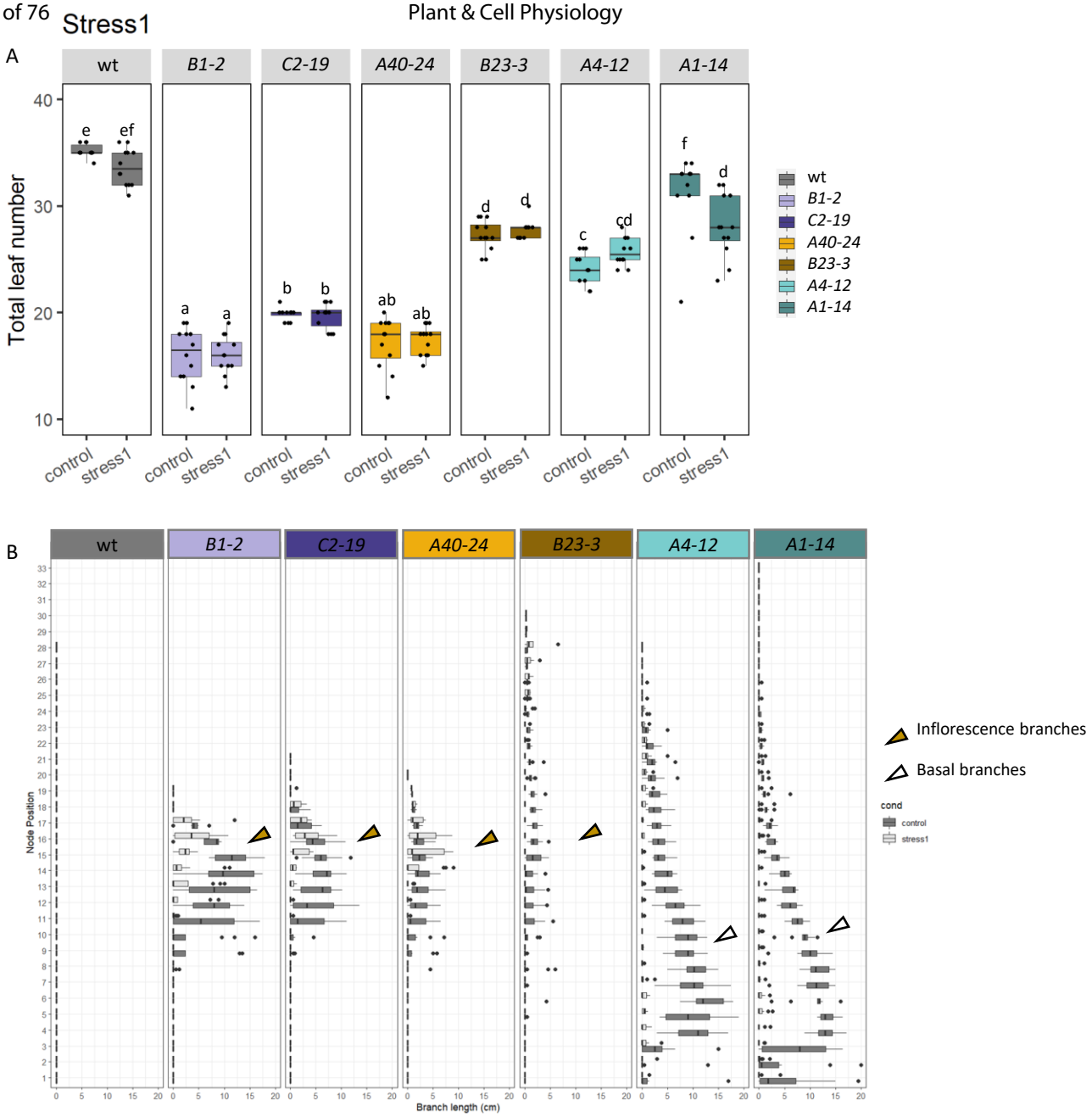

Figure S3: Drought impacted branch length but not the total leaf number

A, Total leaf number of the wt and the *B1-2*, *C2-19, A40-24*, *B23-3*, *A4-12* and *A1-14* mutants in control and in response to drought (stress 1). B, Branch lenght in each node of wt and the *B1-2*, *C2-19, A40-24*, *B23-3*, *A4-12* and *A1-14* plants observed at the end of the 10-day drought stress in the control and in response to drought (stress 1). In B and C, boxes indicate the interquartile range, the vertical line in the middle is the median, the horizontal lines (whiskers) correspond to the highest or lowest value within 1.5 times the interquartile range, letters show significant differences between conditions and genotypes ($p<0.05$, using ANOVA followed by Tukey's pairwise multiple comparisons), n = 10 to 12

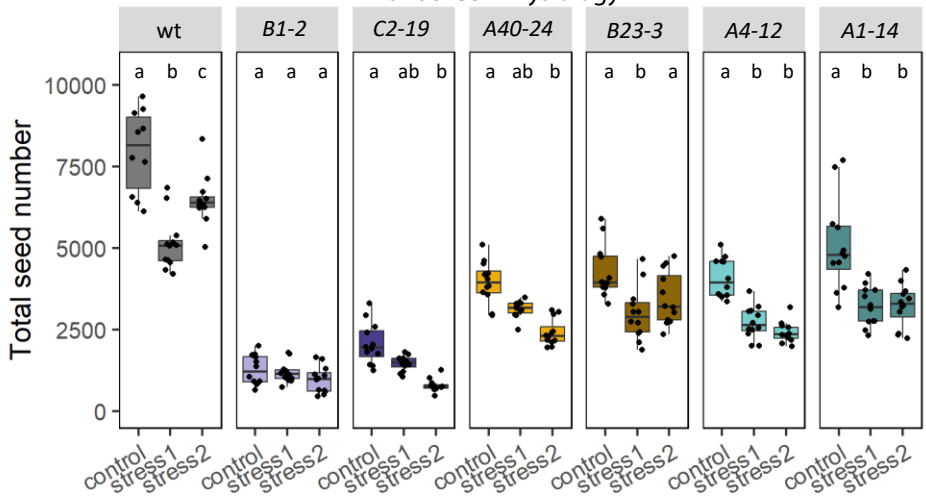

Figure S4: Drought before and after flowering impacted total seed number
Total seed number of wt and the *B1-2*, *C2-19*, *A40-24*, *B23-3*, *A4-12* and *A1-14* plants in control condition and in response to early drought (stress 1) and drought at flowering (stress 2). Boxes indicate the interquartile range, the vertical line in the middle is the median, the horizontal lines (whiskers) correspond to the highest or lowest value within 1.5 times the interquartile range, letters show significant differences between conditions only ($p<0.05$, using ($p<0.05$, using ANOVA followed by Tukey's pairwise multiple comparisons), n = 10 to 12.

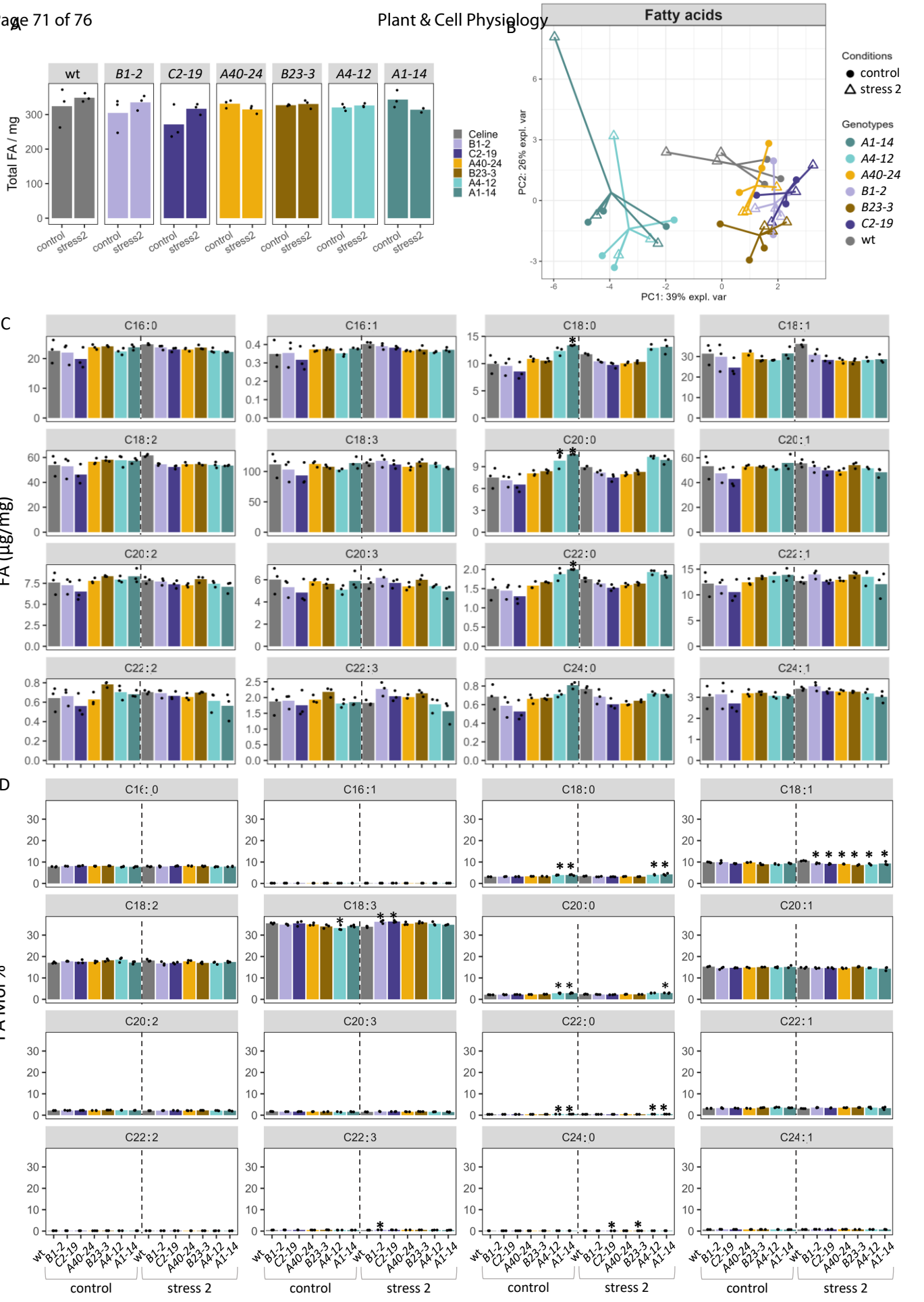
A
wt
B1-2
C2-19
A40-24
B23-3
A4-12
A1-14
Total FA / mg
control
stress2
Celine
B1-2
C2-19
A40-24
B23-3
A4-12
A1-14
B
Fatty acids
PC2: 26% expl. var
PC1: 39% expl. var
Conditions
control
stress 2
Genotypes
A1-14
A4-12
A40-24
B1-2
B23-3
C2-19
wt
C
FA (µg/mg)
C16:0
C16:1
C18:0
C18:1
C18:2
C18:3
C20:0
C20:1
C20:2
C20:3
C22:0
C22:1
C22:2
C22:3
C24:0
C24:1
D
FA Mol %
control
stress 2

Figure S5: Total fatty acid and fatty acid composition showed only few changes in *flo*- mutants in control condition and in response to drought

A, Total fatty acid in mature dry seeds of the wt and the *flo*- mutants (*B1-2*, *C2-19, A40-24*, *B23-3*, *A4-12* and *A1-14)* in control condition and in response to drought at flowering (stress 2). B, Principal component analysis (PCA) showing the positions of samples in the plane delineated by component 1 and 2 accounting for 65% of the total variance of the FAs quantified in mature seeds of the wt and the *flo*- mutants (*A1-14*, *A4-14*, *A40-24*, *B1-2*, *B23-3* and *C2-19*) in control condition (triangles) and in response to stress 2 (circles). C-D, Fatty acid composition in µg/mg (C) and in Mol % (D). In A, C and D, stars indicate significant differences between wt and the *flo*- mutants (*B1-2*, *C2-19, A40-24*, *B23-3*, *A4-12* and *A1-14)* ($p<0.05$, using ANOVA followed by Tukey's pairwise multiple comparisons), n = 10 to 12.

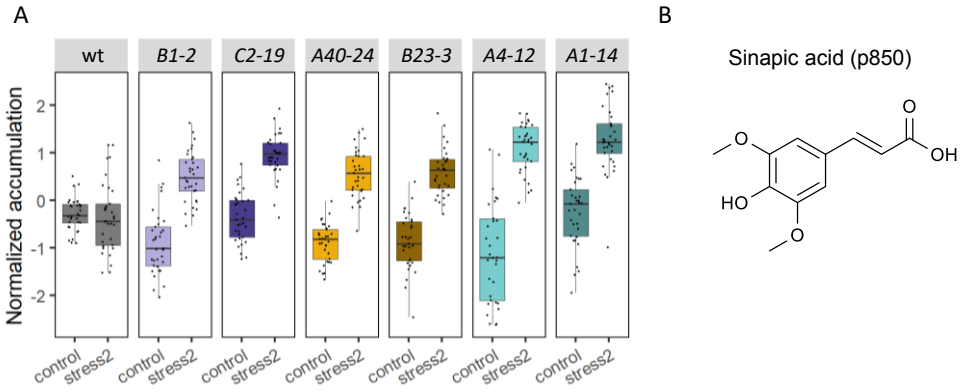

Figure S6: Features that showed an increase in accumulation in all the *flo*- mutants upon drought stress
(A) Normalized accumulation and (B) structure of the annotated putative metabolite of the eleven features significantly accumulated in mature dry seeds upon drought stress (indicated with a red star on figure 4B). In A, boxes indicate the interquartile range, the vertical line in the middle is the median, the horizontal lines (whiskers) correspond to the highest or lowest value within 1.5 times the interquartile range, *n* = 3.

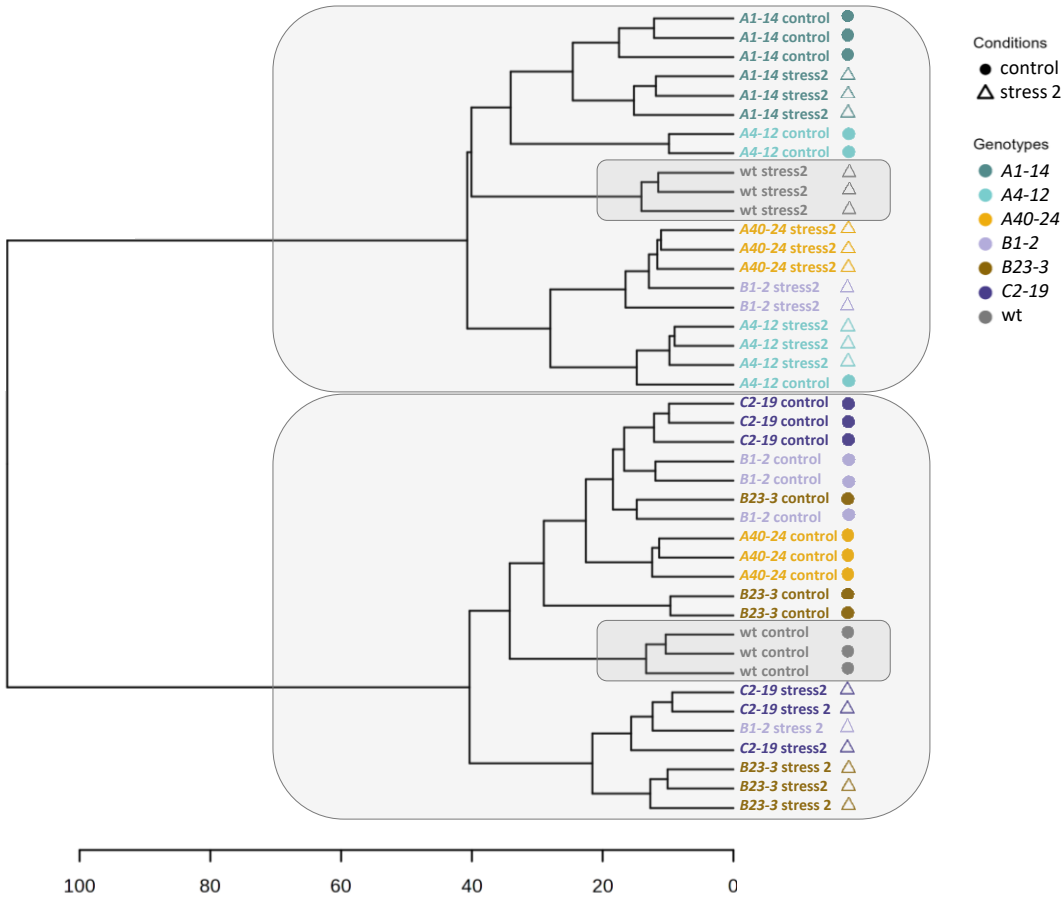

Figure S7: The seed specialized metabolome of the *A1-14* and *A4-12 flo-* mutants showed a constitutive wt stress response while the specialized metabolome of the *C2-19* and the *B23-3 flo-* mutants showed a wt control response upon drought stress.
Hierarchical clustering dendrogram of the 202 features significantly regulated in control condition compared to stress in wt (indicated with a black star on Figure 4B).

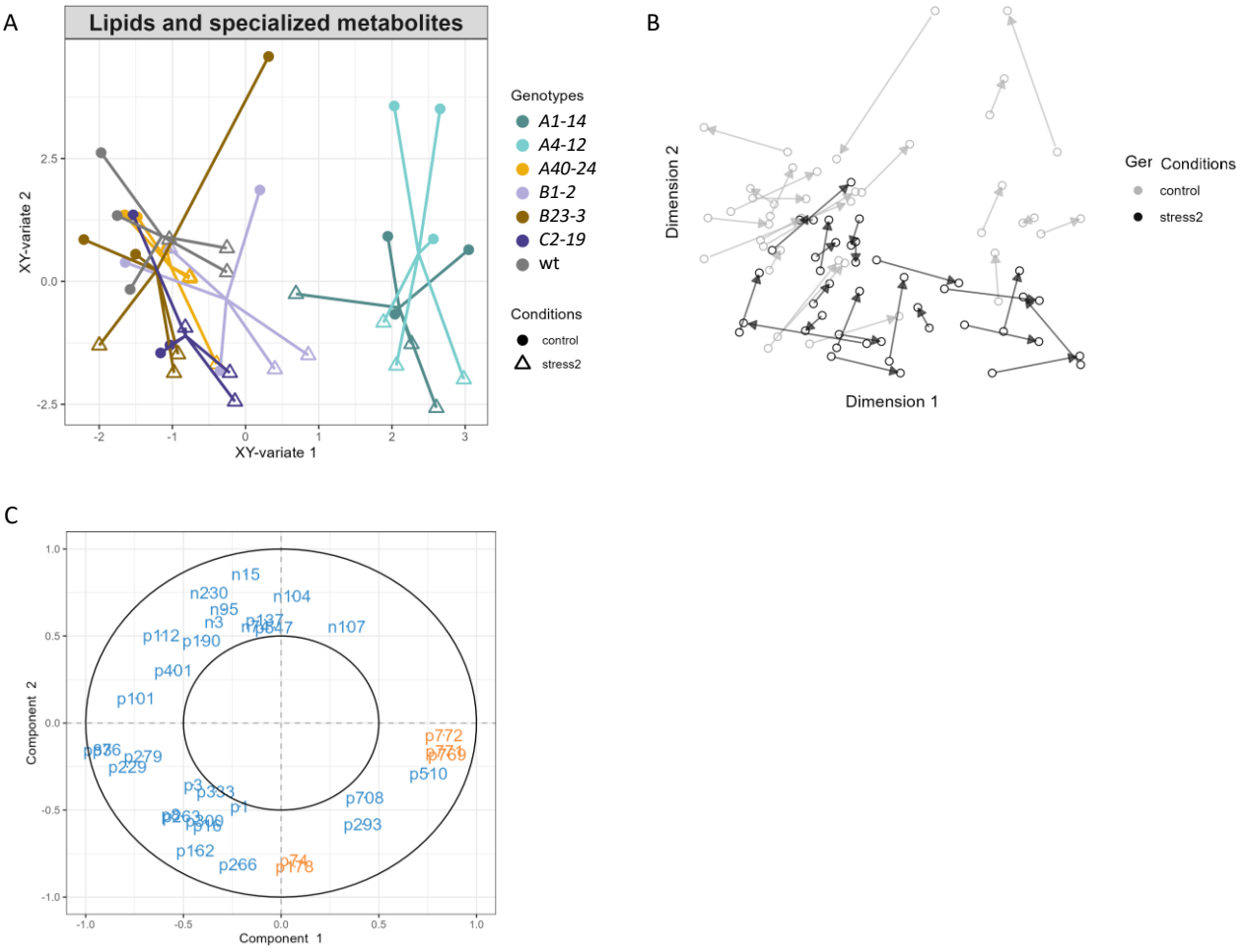

Figure S8: Integration of specialized metabolite and lipid datasets

A, sPLS-DA, that identified and integrated the most discriminative features from lipid and specialized metabolite datasets that best separate the wt and the *flo*- mutants (*B1-2*, *C2-19*, *A40-24*, *B23-3*, *A4-12* and *A1-14*) in control condition and in response to drought at flowering (stress 2) and highlighting correlated features (C). B, Arrow sample plot, showing how each sample project in both lipid and specialized metabolite data. The start and the end of the arrow indicates the sample projection on the two components from the lipids to the specialized metabolites data (Same figure as in Figure 5A with a different color legend). C, Correlation circle plot (correlation coefficient>0.55) with the lipids (blue) and putative specialized metabolites (orange) that are important to define each component of the sPLS-DA (A). Positively correlated variables are grouped together. Negatively correlated are positioned on opposite sides of the plot origin.

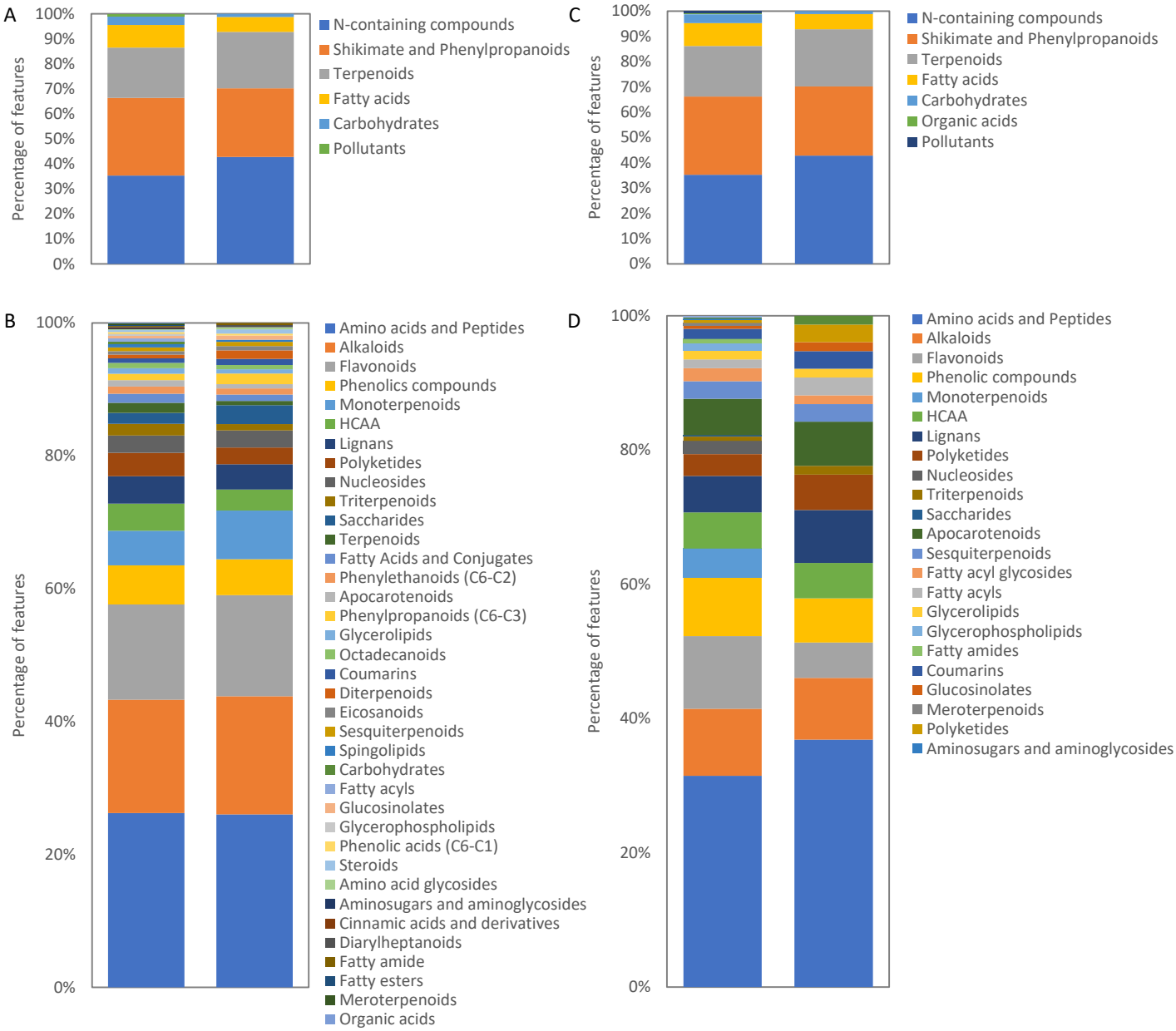

Figure S9: Metabolite families and family groups from total annotated features and the features differentially accumulated across genotypes (wt and the *B1-2*, *C2-19, A40-24*, *B23-3*, *A4-12* and *A1-14 flo*- mutants) in mature seeds and vegetative leaves

A, Percentage of the metabolite families in the 851 (49%) annotated features of the 1739 total features quantified in mature seeds (left) and in the 364 (50%) annotated features of the 725 features identified differentially accumulated in mature seeds across genotypes (wt and the *B1-2*, *C2-19, A40-24*, *B23-3*, *A4-12* and *A1-14 flo*- mutants; right). B, Percentage of the metabolite family group in the 732 (42%) annotated features of the 1739 total features quantified in mature seeds (left) and in the 315 (43%) annotated features of the 725 features identified differentially accumulated in mature seeds across genotypes (wt and the *B1-2*, *C2-19, A40-24*, *B23-3*, *A4-12* and *A1-14 flo*- mutants; right). C, Percentage of the metabolite families in the 545 (60%) annotated features of the 913 total features quantified in vegetative leaves (left) and in the 84 (64%) annotated features of the 132 features identified differentially accumulated in vegetative leaves across genotypes (wt and the *B1-2*, *C2-19, A40-24*, *B23-3*, *A4-12* and *A1-14 flo*- mutants; right). D, Percentage of the metabolite family group in the 464 (51%) annotated features of the 913 total features quantified in vegetative leaves (left) and in the 77 (58%) annotated features of the 132 features identified differentially accumulated in vegetative leaves across genotypes (wt and the *B1-2*, *C2-19, A40-24*, *B23-3*, *A4-12* and *A1-14 flo*- mutants; right).

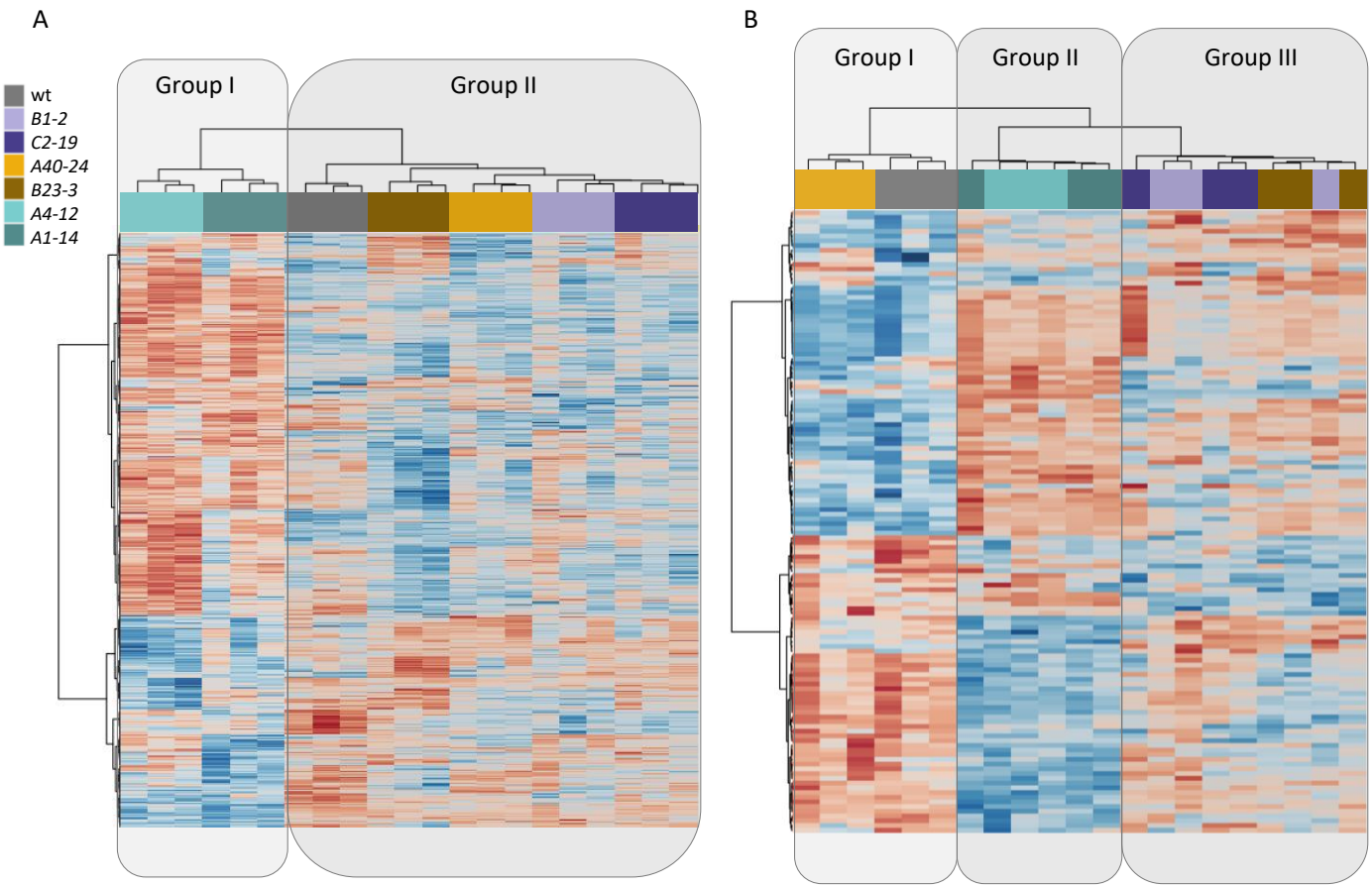

Figure S10: Hierarchical clustering of metabolomic data of the wt and the *B1-2*, *C2-19, A40-24*, *B23-3*, *A4-12* and *A1-14 flo*- mutants showed different groups in seeds and leaves.

A, Heat map representing the hierarchical clustering of the 725 significantly regulated features in the mature dry seeds grown in control condition. B, Heat map representing the hierarchical clustering of the 132 significantly regulated features in vegetative leaves.

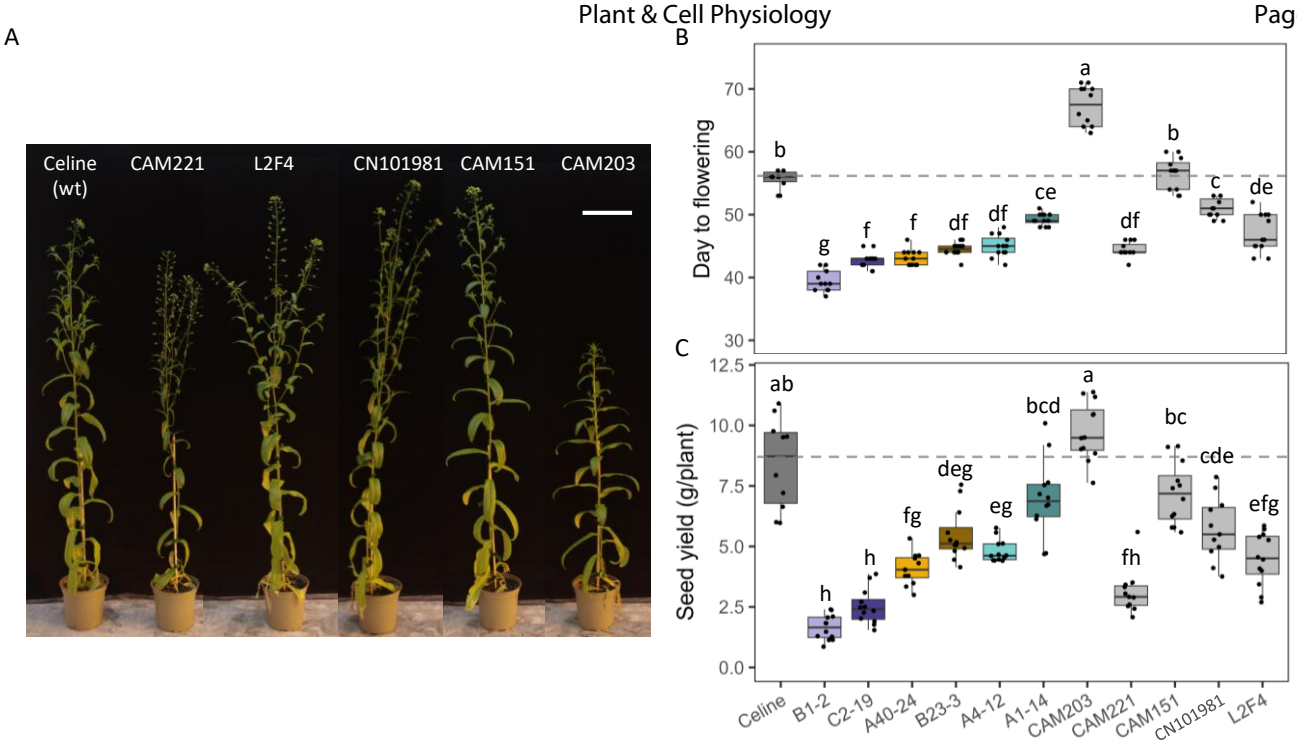

Figure S11: Flowering time and seed yield of the natural accesions with various flowering times
A, Picture of 58 day-old wt (Celine) and the CAM221, L2F4, CN101981, CAM151, CAM203 additional genotypes. Bar, 15-cm. B, Days to flowering (days to the first flower open) of wt (Celine), CAM221, L2F4, CN101981, CAM151 and CAM203. The dotted line indicates the flowering time of the wt (Celine). Boxes indicate the interquartile range, the vertical line in the middle is the median, the horizontal lines (whiskers) correspond to the highest or lowest value within 1.5 times the interquartile range, letters show significant differences between genotypes ($p<0.05$, using ANOVA followed by Tukey's pairwise multiple comparisons), *n* = 10 to 12